buildings

MDPI

Article

Research on Optimization of Climate Responsive Indoor Space Design in Residential Buildings

Zhixing Li [1,*], Yukai Zou [2], Mimi Tian [1] and Yuxi Ying [1]

[1] School of Design and Architecture, Zhejiang University of Technology, Hangzhou 310023, China; tmm518@zjut.edu.cn (M.T.); 2111915071@zjut.edu.cn (Y.Y.)
[2] School of Architecture and Urban Planning, Guangzhou University, Guangzhou 510006, China; zou.yukai@outlook.com
* Correspondence: zxlee910@zjut.edu.cn; Tel.: +86-15375543915

Abstract: This paper first analyzes the climate characteristics of five typical cities in China, including Harbin, Beijing, Shanghai, Shenzhen and Kunming. Then, based on Grasshopper, Ladybug and Honeybee analysis software, according to the indoor layout of typical residential buildings, this research extracts design parameters such as the depth and width of different rooms and their window-to-wall ratios etc., to establish a climate responsive optimization design process with indoor lighting environment comfort, with heating and cooling demand as the objective functions. Meanwhile, based on Monte Carlo simulation data, ANN (Artificial Neural Network) is used to establish a prediction model to analyze the sensitivity of interior design parameters under different typical cities' climatic conditions. The study results show that the recommended values for the total width and total depth of indoor units under the climatic conditions of each city are both approximately 14.97 m and 7.88 m. Among them, under the climatic conditions of Harbin and Shenzhen, the design parameters of residential interiors can take the recommended value of UDI optimal or nZEB optimal. While the recommended values of window-to-wall ratios for the north bedroom, master bedroom and living room in Shanghai residential interiors are 0.26, 0.32 and 0.33, respectively. The recommended value of the window-to-wall ratio of the master bedroom in Kunming residences is 0.36, and that of the remaining rooms is between 0.15 and 0.18. The recommended values of window-to-wall ratios for the master bedroom and living room in Beijing residences are 0.41 and 0.59, respectively, and that for the remaining rooms are 0.15. The multi-objective optimization process based on parametric performance simulation used in the study can effectively assist architects in making energy-saving design decisions in the preliminary stage, allowing architects to have a case to follow in the actual design operation process.

Keywords: climate responsive optimization design; lighting environment comfort; heating and cooling demand; ANN

Citation: Li, Z.; Zou, Y.; Tian M.; Ying, Y. Research on Optimization of Climate Responsive Indoor Space Design in Residential Buildings. *Buildings* **2022**, *12*, 59. https://doi.org/10.3390/buildings12010059

Academic Editor: Natasa Nord

Received: 16 November 2021
Accepted: 3 January 2022
Published: 7 January 2022

1. Introduction

Energy consumption of the construction industry accounts for 40% of the total energy consumption of most countries, and the related emissions account for 40% of the total greenhouse gas emissions [1]. This energy use will potentially grow by more than 50% by 2050 without energy-efficiency improvements in the building sector [2]. In the past two decades (1984–2004), major energy consumption has increased by 49%, carbon dioxide emissions have increased by 43%, and the average annual growth rate is 2% and 1.8% [3]. This speed of resource and energy consumption will affect every aspect of people's daily lives around the world. According to the energy use forecast of different countries and major developed countries, the speed of building energy consumption will

continue to increase, bringing immeasurable serious consequences to nature and ecology. In order to cope with environmental problems, it is necessary to improve the energy efficiency of buildings and promote the use of renewable energy. The research of near-zero energy building (nZEB) has been rapidly developed in this context. Near-zero energy buildings refer to buildings that adapt themselves to climate characteristics and natural conditions. Through adopting envelopes with high thermal insulation and better airtight performance, as well as high-efficiency fresh air heat recovery technology, nZEB aims to minimize the heating and cooling needs of buildings and make full use of renewable energy to provide a comfortable indoor environment with less energy consumption and meets the basic requirements of green building [4]. On 18 June 2010, the European Union issued the "Energy Performance of Buildings Directive" (Agenda 2030), which stipulated that all of the new buildings in the members of EU countries should be near-zero energy buildings since 31 December 2020 [5]. Moreover, EPBD2010 also required that since 31 December 2018, buildings used or owned by the government should be near-zero energy buildings [6]. In 2016, China also released the "Chinese Near-Zero Energy Building Best Practice Cases Collection" to summarize and sort out the technology and construction methods of Chinese existing near-zero energy building projects.

A large number of existing studies have shown that the design phase is of great significance to the realization of near-zero energy buildings, and most building designers lack effective means to evaluate and predict building energy efficiency in the early design stage of the project, which has greatly limited the development of near-zero energy consumption buildings. The focus of energy conservation design in the design phase and subsequent phases is different. The early design phase focuses more on the interaction and influence between the building and the environmental factors. As the design process advances, the subsequent phases will gradually shift focus to the internal mechanical system level. Therefore, the earlier the design phase, the easier to adjust the design factors of the building-environment interaction, and the adjustment of each factor will make a huge difference in the environmental benefits of the building. Therefore, the decision at the schematic stage is an extremely important part of the building energy-saving design process, which largely determines the direction of the subsequent design process.

EPBD pointed out that the building's energy-saving goals cannot be achieved at the expense of indoor comfort. Based on Chinese typical cities in different climatic environments, the research builds a multi-variable and multi-objective optimization design framework, proposes optimal design guidelines for each typical city and summarizes the design rules of residential buildings under different climatic conditions. Using digital tools, professional simulation software widely used internationally and multi-objective optimization algorithm, this study creates a set of systematic parametric analysis processes, which can effectively carry out building climate responsive design in the schematic design stage. Based on the perspective of architects, this paper establishes the relationship between architectural design strategy, building lighting environment and building energy demand, in order to providing architects with low energy demand and high lighting comfort design basis for building climate responsive design. In addition, through the analysis of simulation data, and the comparison of the optimization results with the performance indicators of reference buildings in various cities, it provides a quantitative analysis method for the design decision-making from multiple perspectives of public sector and private residents. Meanwhile, the energy-saving design rules of residential buildings in typical cities under different climate conditions are summarized.

2. Background and Literature

2.1. Literature Review

2.1.1. Building Climate Responsive Design

The design strategy of building climate responsive aims to study the climate control method suitable for building comfort space. By considering the climate differences in different places, appropriate strategies are used to improve the indoor comfort of residents. The building provides a comfortable indoor environment for human daily activities by adjusting the microclimate of the natural environment. In this method, the selection of technology is based on the relationship between external climate conditions and human needs. In the building climate responsive design, architects need to make full use of the potential of natural climate while adapting to the natural environment, and actively and reasonably use various technical measures such as heat preservation, heat insulation, ventilation, shading and daylighting to adapt to the climate characteristics of the region. Table 1 illustrates the literature review of building climate responsive design.

Table 1. Literature review of building climate responsive design.

Authors	Time	Main Work	Reference
V. Olgyay	1953	He first proposed the building climate analysis method which recommended architects to use passive means to adjust the building microclimate in architectural design.	[7]
V. Olgyay	1963	He published "Design with Climate" which proposed to adopt a passive design method to maximize the use of renewable energy such as solar energy and wind energy, as well as reduce building energy consumption.	[8]
Baruch Givioni	1976	He improved Olgyay's bioclimatic chart and proposed architectural bioclimatic design method based on climate environment and distinguished it from Olgyay's method. Architectural bioclimate design requires that, in the process of architectural design, solve the problems of the architectural environment by making use of natural conditions as much as possible, propose corresponding architectural technical means and control methods, and create a more comfortable and healthier environment that meets the requirements of modern society on the basis of respecting the nature environment.	[9]
Alsousi et al.	2005	They studied the climate responsive design of buildings in Gaza and investigated 12 high-rise residential buildings in terms of thermal comfort and energy consumption. The researchers finally found that most of the building energy consumption in summer is caused by the heat generated by the walls, windows and roof. In addition, the occupants, daily life facilities and air infiltration will also increase the building energy consumption, while the effect of them on the thermal performance and occupants' comfort are relatively small.	[10]
Enedri et al.	2007	They tested the thermal performance of a multi-story residential building in southern Brazil. They recorded the thermal performance of eight bedrooms on two floors and four directions. Different variables are used to examine various factors, such as surface color, window shadow and thermal properties of walls and windows. Finally, it is concluded that the heating transmittance and area of the building envelope have the greatest influence on the maximum temperature, and it needs to be minimized to improve the indoor thermal environment in summer. While heat capacity and thermal time lag have the strongest correlation with the minimum temperature, so they	[11]

		should be maximized to improve the thermal environment comfort in winter.	
Jürgen schnieders et al.	2015	They used the same typical analysis model to analyze and compare the design strategies of passive housing, including envelope design, air tightness, operation of cooling coil, heat recovery equipment and supply air temperature, etc., taking Yeka-Tlinburg, Tokyo, Shanghai, Las Vegas, Abu Dhabi and Singapore as examples, to propose the corresponding design guidelines for passive buildings.	[12]
Letizia Martinelli et al.	2017	They selected six Italian cities as representatives, including Aosta, Milan, Campobasso, Florence, Lecce and Catania. Based on the climate data of each city in the past 30 years, the influence of courtyard-type parameters such as the ratio of height to width on the humidity and thermal comfort of the courtyards of various cities in different climate zones is analyzed.	[13]
Fatima Harkooss et al.	2018	They selected 25 typical cities in different climate regions to simulate and optimize the passive design of residential buildings according to the Köppen climate zoning. He compared the performance of residential buildings in different cities by taking the life cycle cost (LCC) and building cooling and heating consumption as objective functions, to obtain the corresponding energy-saving design strategy.	[14,15]
Fabrizio Ascione et al.	2019	They used MATLAB, EnergyPlus and genetic algorithm to compare the multi-objective optimization of residential buildings in typical cities in different climates in Italy and obtained the envelope design strategy for each climate zone.	[16]
Julià Coma et al.	2019	Based on the European residential building database compiled by the TABULA/EPISCOPE project, they analyzed and compared the energy-saving strategies of many European countries with building energy consumption and carbon dioxide emissions as indicators. They also evaluated the feasibility of using new energy technologies in different cities in hot, warm and cold climate zones in Europe.	[17]
Virgilio Ciancio et al.	2020	They discussed the impact of climate warming on residential buildings in 19 different cities in Europe based on the Köppen climate zoning. They concluded that the gradual increase of average climate temperature from 2050 to 2080 will lead to the decrease of heating energy consumption of residential buildings, and the increase of cooling energy consumption and carbon dioxide concentration. Moreover, cities in the Mediterranean climate zone are more affected by global heating than inland cities in Europe. This trend can be alleviated by improving the buildings' energy efficiency.	[18]

2.1.2. Multi-Objective Optimization

As mentioned above, this study proposes the use of optimized search methods based on building environment simulation. Optimization is the process of finding the best combination of different solutions when the given constraints are met [19]. The execution of optimization requires decision variables, objective functions and constraints. Equation (1) expresses the general mathematical optimization process:

$$\begin{gathered} \min_{x \in Rn} f(X) \\ \text{Subject to: } g_i(X) \le 0,\ i = 1, 2, \ldots, m \\ K_j(X) = 0,\ j = 1, 2, \ldots, p \end{gathered} \quad (1)$$

where X represents different decision variables, $f(X)$ are objective functions, constraints are $g_i(X) \le 0$, i = 1, 2, ..., m and $K_j(X) = 0$, j = 1, 2, ..., p. Determining decision variables, objective functions and constraints are the most important parts of the optimization process, and different optimization algorithms can be selected based on the classification of different objective functions and constraints.

According to Kheiri [20], the most widely used optimization method for building energy performance problems is the genetic algorithm (GA) [21]. John Holland has developed genetic algorithms (GAs) based on evolutionary biology, which perform optimization operations by simulating genetics, mutation, selection and crossover. [22] The evolution of genetic forms is based on the rules of the defined "genetic code". Mutations are achieved through the "reproduction" process of gene crossover and mutation. Information interaction and changes control the process of morphogenesis. The use of genetic algorithms in the first step is to define a set of generation rules and define their evolution and development so that they can be mapped to a specific design environment, and candidate forms can be evaluated based on their performance in a simulated environment. After a lot of tests, researchers believe that genetic algorithms are suitable for searching research problems in large spaces, while also avoiding local optimization.

The early algorithms mainly focused on single-objective optimization [23–25]. However, the research results of some scholars show that there are conflicts between different optimization goals, and the single-objective optimization cannot achieve satisfactory results. Therefore, there are several studies which focus on the multi-objective optimization of buildings' performance, as shown in Table 2.

Table 2. Literature review of building performance simulation based on multi-objective optimization.

Authors	Time	Main Work	Reference
Chantrelle et al.	2011	They used NSGA-II algorithm (Non-dominated Sorting Genetic Algorithm) and dynamic simulation tool TRNSYS to carry out multi-objective optimization design of building envelope and shading control strategy based on building energy consumption, cost, thermal comfort and environmental protection.	[26]
Karaguzel et al.	2014	They combined the building energy simulation software EnergyPlus and the optimization tool GenOpt to optimize the life cycle cost of a commercial office building.	[27]
Alessandro Prada	2014	They implemented a comprehensive framework of multi-objective energy optimization in buildings, and used EnergyPlus and NSGA-II algorithm for building environment simulation and multi-objective optimization to search Pareto frontier for building energy-efficiency design.	[28,29]
Ascione, F. et al.	2014	They combined MATLAB and EnergyPlus to optimize the construction plan of a hospital building with multiple goals. The optimization goals	[30]

		are the primary energy consumption of the building, the initial investment and global cost of the renovation plan.	
Asl et al.	2015	They presented an integrated framework for building information modeling (BIM)-based performance optimization, BPOpt.	[31]
Tomás Méndez Echenagucia	2015	An integrative approach for the early stages of building design is proposed to obtain detailed information on energy-efficient envelope configurations.	[32]
Facundo Bre et al.	2016	They took daylighting and energy saving as optimization goals, and used sensitivity analysis and genetic algorithms to optimize the design of typical independent houses.	[33]
Ahmed Toutou et al.	2018	They discussed the potential of parametric algorithms to optimize residential design lighting and thermal performance.	[34]
Richard Gagnon et al.	2019	Through a case study of a residential building, they compared a sequential versus a holistic design approach based on multi-objective optimization.	[35]
Yin Li et al.	2019	They proposed a hierarchical decomposition approach that can achieve global optimal solutions. This approach was applied to a multi-objective optimization problem to minimize the carbon emissions and operating costs of buildings.	[36]
Tianqi Zhang et al.	2020	This research calculated the energy-saving effect of buildings with different shape parameters and the cooling load of thermal performance of different envelope by numerical simulation. In addition, the corresponding energy-saving indexes for cooling load reduction (CLR) are presented.	[37]
Zhixing Li et al.	2021	They proposed an integrated multi-objective multivariate framework for building performance optimization. Then, a comparison of the performance indicators of low-rise and medium-rise residential buildings under five typical urban climatic conditions are carried out.	[38]
Yizhe Xu et al.	2021	They proposed a two-stage multi-objective optimization method based on a meta-model to obtain the optimal design scheme for primary and secondary school education buildings, based on daylighting, thermal comfort, energy savings and economy.	[39]

2.1.3. Research Gap

The research on residential building climate responsive design has shown a trend of gradual deepening and refinement over time, which is reflected in the following characteristics:

1. Transition from energy-saving design practice or theoretical research based on qualitative analysis to quantitative research based on energy consumption simulation.
2. The research related to building energy consumption is becoming more and more comprehensive, from only focusing on the thermal performance of buildings or the energy consumption of heating and cooling systems to comprehensive assessments that also consider other factors such as total building energy consumption, lighting and indoor thermal comfort.
3. "Performance coupling factors" are valued. The development of society and economy requires sustainable building design to achieve low energy consumption under the premise of ensuring high performance building environment, and "high performance" cannot be sacrificed for low energy consumption. As the pursuit of single-environment performance improvement often has an adverse effect on other

aspects of performance, research on multiple environments and their coupling performance has attracted more and more attention.

4. New tools or new methods for building performance simulation such as BIM technology or computer programming technology are constantly emerging. On this basis, the amount of simulated data is increasing and the reliability of simulation results is improving.

However, current research still pays more attention to the building equipment optimization, while ignoring the influence of passive design parameters such as the building space form in the preliminary design stage on energy saving. As the schematic design stage has a far-reaching impact on building energy efficiency, and the flexibility of adjustment is greater than other design stages. If the energy-saving benefits and climate responsiveness of the building are ignored in the early stage of the design, it is difficult to compensate for the energy-saving efficiency of the building only through technical stacking and parameter adjustment of active equipment in the later stage. Therefore, this article will take the residential indoor space form design as the research object and conduct an in-depth discussion on the residential building climate responsive design in different regions in China.

2.2. Typical Cities' Selection

China is located on the west coast of the Pacific Ocean. The climate is mainly affected by the monsoon circulation, and it is complicated due to the variability of the terrain. It is roughly divided into the eastern monsoon area, the western dry area and the alpine area with the Gangdise Mountains, Bayan Har Mountains, Yinshan Mountains, Helan Mountains and Daxingan Mountains as the boundary. Taking Kunlun Mountains, Altun Mountains, Qilian Mountains and Hengduan Mountains as the approximate geographic boundaries, the northwest arid and semi-arid regions, the eastern monsoon regions and the Qinghai-Tibet alpine regions are distinguished [40].

In the "Code for Thermal Design of Civil Buildings GB50176-93" promulgated in 1993, China divided the country into 7 first-class building climate zones and 20 second-class building climates based on the average temperature of the coldest and hottest months across the country. The first-class climate zone reflects the big difference in the national building climate, as shown in Figure 1, while the secondary zone reflects the small differences in the building climate of each major zone.

Figure 1. Chinese building climate zoning map.

According to the building climate division in China, five typical cities are selected from climate zones I, II, III, IV and V, which are Harbin (severe cold region I), Beijing (cold region II), Shanghai (hot summer and cold winter zone III), Shenzhen (hot summer and warm winter zone IV) and Kunming (temperate area V), as shown in Figure 2.

China divides the heating area with the Qinling mountain and Huaihe River as the boundary. The area north of the Qinling mountain and the Huaihe River starts to centralize heating around November 15th and lasts for 4 months until March 15th. Some areas (such as Harbin and other northern cities) will extend the heating period due to climatic reasons. There are no mandatory centralized heating measures for cities on the south of the Qinling mountain and the Huaihe River, however, some communities will provide heating according to actual needs. Table 3 lists the heating period of typical cities based on the current actual heating situation survey in various cities.

Due to the vast land area of China and the influence of different factors such as altitude, topography, coastal or inland areas, the climate in different regions varies greatly. Among these five typical cities, the average relative humidity of Beijing and Harbin is relatively low. From January to April each year, the average relative humidity of Beijing and Harbin fluctuates around 40%. Regarding the average dry bulb temperature, except for Kunming, where the annual temperature changes are relatively gentle, the coldest month is about 10 °C and the hottest month is about 30 °C. The average dry bulb temperature among the other four cities basically shows a trend of gradual decrease from south to north. The coldest months in Harbin are January and December each year and the average dry bulb temperature can reach −15 °C.

Figure 2. Geographical location of typical cities in China.

Table 3. Typical cities selected according to building climate zoning.

Climate Zone	Typical City	Heating Degree Day (18 °C)	Heating Period (Day/Month)	Heating Hours per Day
Severe cold area I	Harbin	≥3800	20/10 to 15/4	24 h
Cold region II	Beijing	2000–3799	15/11 to 31/3	24 h

Hot summer and cold winter area III	Shanghai	700–1999	There is no mandatory requirement	–
Hot summer and warm winter area IV	Shenzhen	<500	There is no mandatory requirement (according to the actual demand, heating time is not set in the simulation)	–
Temperate region V	Kunming	<2000	There is no mandatory requirement (but it is set to 15/12 to 1/3 in the simulation according to the actual demand)	–

3. Multi-Objective Model Set-Up

3.1. Building Performance Optimization Workflow

Grasshopper and Ladybug/Honeybee were used in this study to achieve building performance simulation-based optimization. Grasshopper is a visual programming language and environment that runs within the Rhinoceros 3D computer-aided design (CAD) application. Ladybug and Honeybee is a plug-in of Grasshopper, which analyzes the environmental performance of the building model [41–43]. Ladybug imports standard RADIANCE, energy models using OPENSTUDIO and envelope heat flow using THERM. This study applied integrative building performance simulation and optimization workflow as shown in Figure 3. TT toolbox and Octopus, as Grasshopper plug-ins were used for collecting dynamic simulation results by Ladybug and Honeybee which was then analyzed via MATLAB for understanding the data distribution characteristics.

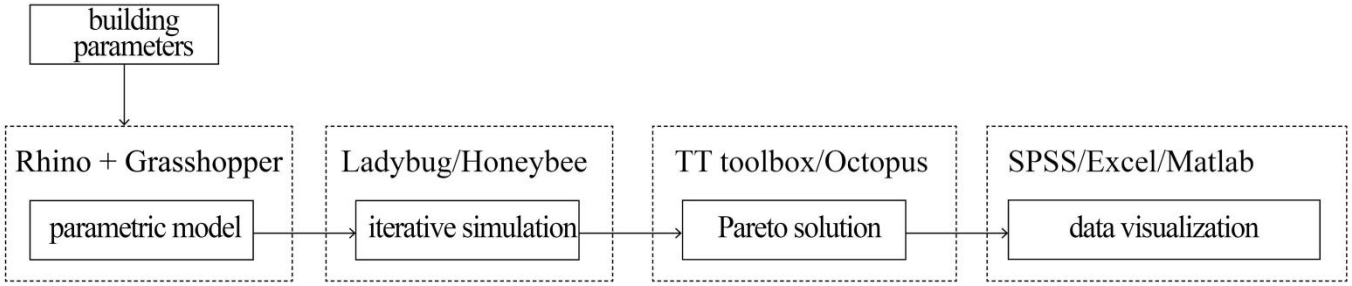

Figure 3. Parametric building optimization process.

3.2. Building Parameter Settings

The study takes the 118.11 square meter apartment in one of Tianjin residential communities as an example to optimize the internal space design parameters. The reference building is shown as Figure 4, its parameters are listed in Table 4, and Figure 5 depicts the apartment layout for optimization analysis. The parametric model is established based on the house type on the left. The house type includes three bedrooms, one living room and one dining room, two bathrooms and a kitchen. The bedrooms are mainly distributed on the west side of the room. The master bedroom faces south and has a separate bathroom. The second bedroom faces north and the middle bedroom is smaller which can also be used as a study room. The living room is connected to the dining room, there is a balcony on the south side, and the kitchen is connected to the dining room on the north side.

The parameter settings used for optimization are shown in Table 5. Under the changes of different spatial parameters, the model always maintains a total area of 118 square meters, that is, it satisfies the relationship of Equations (2)–(4). In the parametric model, as the parameters in Table 5 change, the spatial scale of the apartment also changes, as shown in Figure 6, and the Grasshopper operation process is shown in Figure 7.

Master bedroom depth + Middle bedroom depth + Northern bedroom depth
= Kitchen/Dining room depth + Living room depth (2)
= Total depth

Master bedroom width + Living room width + 1.8 m (Toilet width)
= Northern bedroom width + 1.8 m (Toilet width) + Dining room width + Kitchen width (3)
= Total width

Total depth × Total width = 118 (4)

Figure 4. Baseline model.

Table 4. Parameters of the baseline model.

Type	Subcategory	Parameter Category	Unit	Baseline Model
Geographical position	Climate	Climate data of Tianjin	–	Climate data of Tianjin
Architectural form parameters	Building type	Number of layers	–	2.00
		Net height of each floor	m	3.30
		Total height of each floor	m	3.60
		Width (s/N direction)	m	13.5
		Aspect ratio	–	2.15
		Window-to-wall ratio (WWR)	–	0.35
		orientation	deg	0
	Geometry parameters	volume	m^3	3089.5
		Total surface area	m^2	1336.4
		Total floor area	m^2	668
		Body shape coefficient	–	0.325
Design parameters of envelope	Enclosure structure	External wall heating transmittance (average)	$W/(m^2K)$	0.56
		Ground heating transmittance	$W/(m^2K)$	0.46

		(average)		
		Roof heating transmittance (average)	W/(m²K)	0.71
		Window heating transmittance (average)	W/(m²K)	3.30
		Solar heat gain coefficient (shading coefficient)	–	0.60
	behavior	Indoor heat gain (lighting, appliances and occupancy, daily average)	W/m²	5
Building operation parameters	Control and operation settings	Heating set point temperature	°C	20
		Cooling set point temperature	°C	26
		Air change rate (air tightness and ventilation)	vol/h	0.8
		Schedule—Option 1: Ig/VE/H/C *	N.	0
		Schedule—Option 2: Ig/VE/H/C *	N.	0/0/1/2

* Ig: indoor heat gain, VE: ventilation, H: heating, C: cooling.

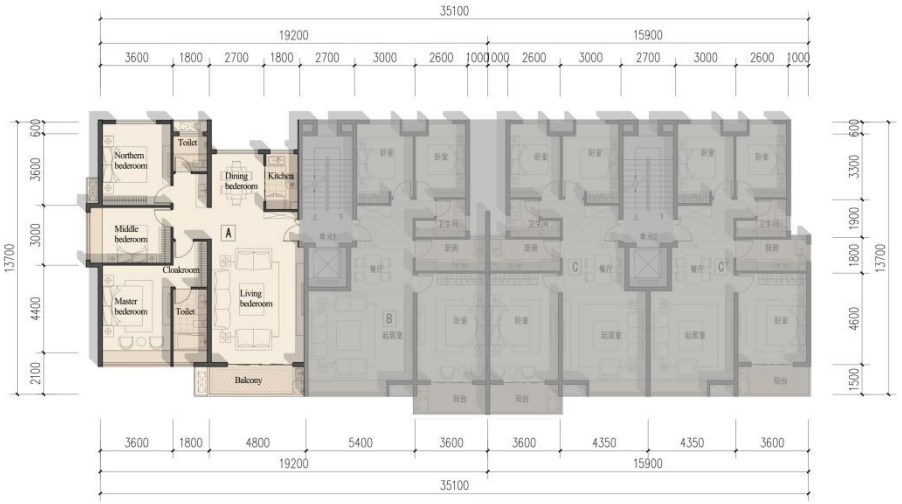

Figure 5. Indoor apartment.

Table 5. Interior space design parameter settings for optimization.

Classification	Number	Describe	Unit	Reference Parameter	Minimum Value	Maximum Value
Spatial morphological parameters	A1	Floor height	m	3	2.7	3.3
	A2	Total width	m	10.2	8	15
	A3	Total depth	m	13.7	7.8	14.8
	A4	Master bedroom width	m	3.6	2.5	5
	A5	Master bedroom depth	m	4.4	2.5	6.5
	A6	Middle bedroom width	m	3.6	2.5	5
	A7	Middle bedroom depth	m	3	1.7	5
	A8	North bedroom width	m	3.6	2.5	5
	A9	North bedroom depth	m	4.2	1.7	6.5
	A10	Kitchen width	m	1.8	1.7	5
	A11	Kitchen depth	m	3	1.7	6.5
Window parameters	B1	Window-to-wall ratio in north bedroom	–	0.35	0.15	0.6

B2	Window-to-wall ratio in middle bedroom	–	0.3	0.15	0.6
B3	Window-to-wall ratio in master bedroom	–	0.35	0.15	0.6
B4	Window-to-wall ratio in living room	–	0.55	0.15	0.6
B5	Window-to-wall ratio in Kitchen	–	0.3	0.15	0.6
B6	Window-to-wall ratio in dining room	–	0.35	0.15	0.6

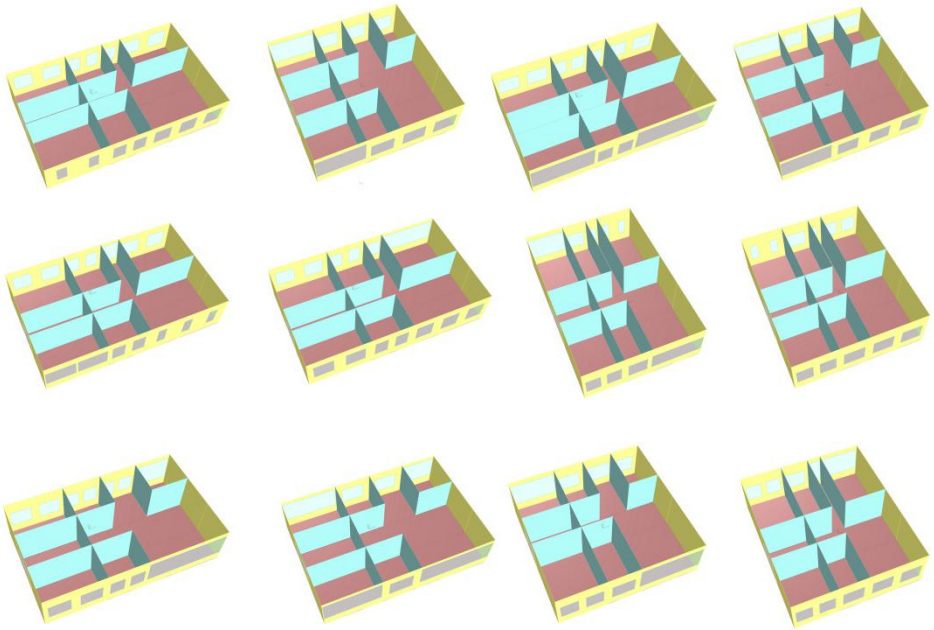

Figure 6. Internal space model (partial) with the parameter changes.

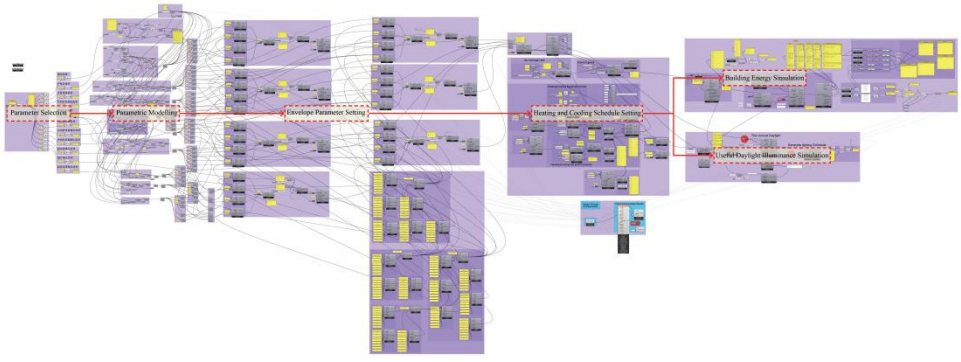

Figure 7. Grasshopper procedure.

In order to compare the optimization results of typical cities in different climate zones with the reference model, and to understand the improvement of the optimization results on the reference model, Table 6 lists the performance indicators of the reference model.

Table 6. Performance indicators of the reference model.

Objective Function	Harbin (Severe Cold Area I)	Beijing (Cold Regions II)	Shanghai (Hot Summer and Cold Winter Area III)	Shenzhen (Hot Summer and Warm Winter Area IV)	Kunming (Temperate Region V)
BED(kWh/m²): Building energy demand	179.42	114.81	85.16	65.20	36.10
H(kWh/m²): Heating energy demand	174.31	97.14	60.21	0	26.03
C(kWh/m²): Cooling energy demand	5.11	17.67	24.95	65.20	10.07
UDI 100–2000(%): Useful Daylight Illuminance	56.58	59.75	60.75	64.67	67

3.3. Objective Function Settings

The evaluation indicators of building climate responsive design include lighting environment comfort and building energy demand. In order to facilitating the parametric modeling and analysis, this section explains the theoretical basis of these two objective functions and clarifies the relevant design influence factors.

3.3.1. Building Energy Demand

The annual building energy demand is defined as the sum of the cooling and heating loads of all apartments [44–46]—domestic hot water, electrical equipment and other energy needs are not included in the calculation. The cooling period in summer and the heating period in winter are set according to the requirements of different climate zones. In this study, in order to avoid the influence of HVAC system parameters, its performance coefficient is assumed to be 1, so the energy demand can be directly extracted from the EnergyPlus simulation results. It is assumed that no heat recovery device is implemented in the HVAC system. Therefore, the objective function of the annual building energy demand can be calculated as Equation (5):

$$BED = 1/A \times \sum^{n}_{i=1}(E_{ci} + E_{hi}) \quad (5)$$

where BED represents the annual building energy demand per unit building area (kWh/m²)—the calculation of building energy demand only considers heating and cooling demand, and does not consider other aspects, such as lighting, domestic hot water, etc. E_{ci} is the cooling demand of the i-th floor, E_{hi} is the heating demand of the i-th floor, n is the total number of floors in the building and A is the total area of each floor in the air-conditioning area of the building.

3.3.2. Lighting Environment Comfort

There are currently two types of light environment evaluation indicators, which are divided into static indicator and dynamic indicator. The static indicators include illumination, uniformity of illumination (U_0), Daylight factor—DF, Unified Glare Rating—UGR and Scope of View. The static lighting environment evaluation index is simple, intuitive and easy to calculate. It is suitable for index control under general conditions, but it cannot distinguish the difference in lighting environment performance under the influence of different climatic factors, and it cannot distinguish the different types of buildings; moreover, it is impossible to evaluate various technical measures such as an auxiliary lighting system. Whereas the dynamic daylighting evaluation indicators including Daylight Autonomy (DA), Continuous Daylight Autonomy (DAcon) and Useful Daylight Illuminance (UDI) take into account the characteristics of different climate zones. It takes one hour as the step length to reflect the annual illuminance level, which is close to the actual situation. The practicability of dynamic daylighting evaluation

indicators is significantly better than that of static indicators. Such indicators not only consider the role of daylighting auxiliary systems, but also evaluate their advantages and disadvantages, thereby providing support for low-energy design [47].

This study uses the lighting environment evaluation index as one of the optimization objectives and conducts a coupling analysis with the building's annual cooling and heating demand. The dynamic daylighting evaluation index is more convenient to evaluate the design parameters from the time scale of the whole year, which is in line with the purpose of this study. Therefore, this study uses the Useful Daylight Illuminance (UDI) as the index of lighting environment optimization. The UDI indicator is mainly used to evaluate the dynamic lighting quality of indoor spaces, and takes into account the part where the actual illuminance of the indoor working surface exceeds the design illuminance at a certain time and may cause glare. This indicator expresses a range value. Within this range, the surface illumination level meets the requirements of indoor work. Nabil and Mardaljevic [48] proposed the effective illuminance range value in 2005: 100 lx < UDI < 2000 lx, below 100 lx indicates that the indoor working surface illuminance is seriously insufficient, and 2000 lx or more may cause glare, which will adversely affect the indoor light and heat environment. Therefore, the UDI of residential buildings should be divided into three intervals, namely, the annual percentage of 100 lx and below, 100–2000 lx, and 2000 lx and above to evaluate the indoor light environment quality.

3.4. Multi-Objective Optimization Algorithm

The basic idea of the NSGA-II algorithm is: first, randomly generate an initial population of size N, and after non-dominated sorting, the first generation of offspring population is obtained through the three basic operations of genetic algorithm selection, crossover and mutation. Secondly, starting from the second generation, merge the parent population with the offspring population for fast non-dominated sorting. At the same time, the crowding degree is calculated for the individuals in each non-dominated layer, and suitable individuals are selected according to the non-dominated relationship and the crowding degree of the individuals to form a new parent population. Finally, a new offspring population is generated through the basic operations of genetic algorithm and so on, until the conditions for the end of the program are met [49–52]. The program flow chart is shown in Figure 8 below.

Assuming that the population is P, the algorithm needs to calculate two parameters Np and Sp of each individual p in P, where Np is the number of individuals dominating individual p in the population, and Sp is the set of individuals dominated by individual p in the population. The total computational complexity of these two parameters is O (Mn2).

The main steps of the algorithm are as follows: (1) find all the individuals with np = 0 in the population and save them in the current set Fl, (2) for each individual i in the current set Fl, its dominating individual set is Si, for l in Si, execute nl = nl − 1, if nl = 0, then save individual l in set H, (3) the individual obtained in Fl is the individual in the first non-dominated layer, and H is used as the current set, and the above operation is repeated until the entire population is classified

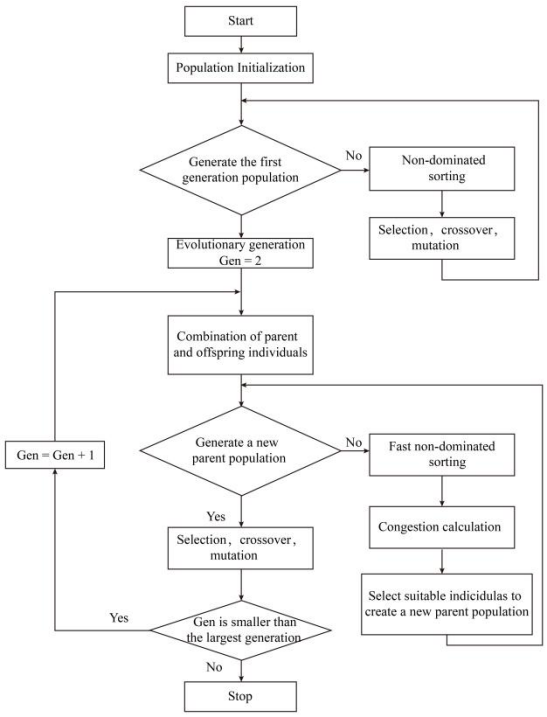

Figure 8. NSGA-II algorithm flow chart.

In order to estimate the crowding degree of the solutions around a particular solution in the population, NSGA-II algorithm calculates the average distance between the two points on both sides of this point according to each objective function. This value is used as an estimate of the perimeter of a box with its nearest neighbor as its vertex (known as the crowding factor) [53]. In Figure 9 below, the crowding factor of the i-th solution at its front is the length of the cuboid around it (as shown by the dashed box). The calculation of the crowding factor ensures the diversity of the population.

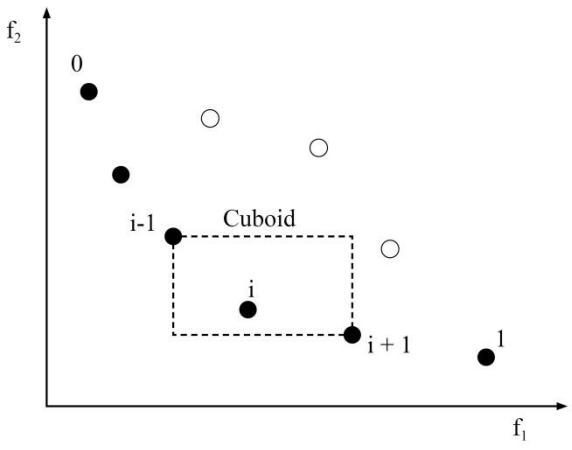

Figure 9. Schematic diagram of crowding factor.

The calculation of the crowding factor needs to sort the populations according to the ascending order of the value of each objective function (that is, if the first-level non-dominated layer is obtained, it is sorted according to the value of the objective function, and then the crowding degree is calculated). Therefore, for each objective function, the boundary solution (the solution with the maximum and minimum values) is specified as the value of the infinite distance. All other intermediate solutions are designated as the normalized absolute difference of the function values of the two adjacent solutions. The

calculation method is the same for other objective functions. All the crowding factor values are calculated by the sum of the distance values of each individual target, and each objective function is normalized before calculating the crowding factor.

In the non-dominated sorting genetic algorithm of elite strategy, the calculation of crowding factor is an important link to ensure the diversity of population. The pseudo code of its function is as follows:

(1) Let nd = 0, n = 1, 2, ... N
(2) For each objective function
    1. The population was ranked based on the objective function,
    2. Let the crowding degree of two individuals on the boundary be infinite, that is, ld = nd = ∞,
    3. Calculate nd = nd + (fm(i + 1) − fm(i − 1)), n = 2, 3, ..., N − 1

After the fast non-dominated sorting and crowding factor calculation, each individual i in the population has two attributes: the non-dominated order irank (i.e., the rank) and the crowding degree id. According to these two attributes, the crowding degree comparison operator can be defined, i.e., individual i compares with another individual j, and as long as any of the following conditions are met, individual i wins.

(1) If irank < jrank
(2) If they have the same rank and individual i has a larger crowding distance than individual j, i.e., irank = jrank and id > jd

The first condition ensures that the selected individual belongs to the superior non-inferior rank. The second condition selects the individual who is located in the less crowded area (having a greater crowding degree id) among the two individuals who are in the same non-inferior rank and who are indifferent due to their crowded distance. The winning individual enters the next operation.

The NSGA-II algorithm adopts the elite strategy shown in Figure 10 [54]. First, the new population Q_t produced by the t th generation and the parent P_t are combined to form R_t, and the population size is 2N. Then, R_t performs non-dominated sorting, generates a series of non-dominated sets Z_i and calculates the crowding factor. Since both offspring and parent individuals are included in R_t, the individuals included in the non-dominated set Z_1 after non-dominated sorting are the best in R_t; so first put Z_1 into the new parent population P_{t+1}. If the size is less than N, then continue to fill the next-level non-dominated set Z_2 into P_{t+1}, until the size of the population exceeds N when Z_3 is added. The crowding degree comparison operator is used for the individuals in Z_3 to make the number of individuals in P_{t+1} reach N. Then a new offspring population Q_{t+1} is generated through genetic operators (selection, crossover, mutation).

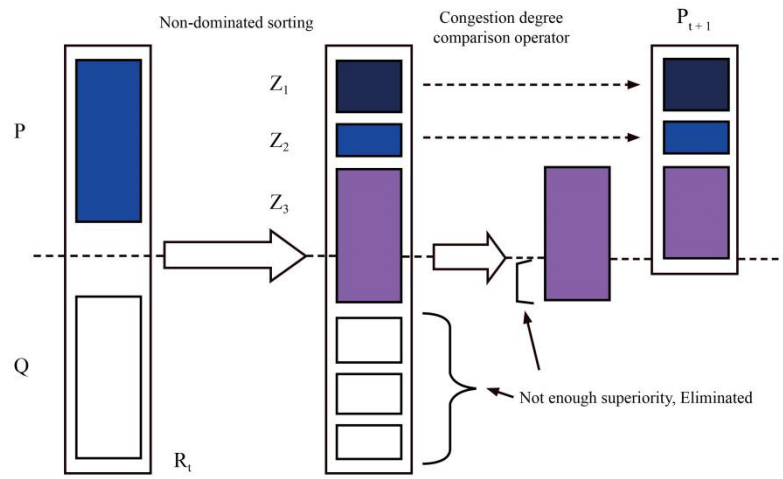

Figure 10. Schematic diagram of elite strategy.

4. Predictive Model Set-Up and Sensitivity Analysis

4.1. Artificial Neural Network Theory

Artificial Neural Network (ANN) is usually called neural network, which is an information processing system that imitates the structure and function of the human brain [55,56]. The establishment of artificial neural networks is based on the collection of connected units or nodes of artificial neurons, which can loosely model neurons. Each connection is like a synapse in a biological brain. It can transmit signals to other neurons. The artificial neurons that receive the signals then process them and send signals to connected neurons. The output of each neuron is calculated by a nonlinear function of the sum of its inputs. Neurons usually adjust their weights as they learn. The increase or decrease of the weight affects the strength of the signal at the connection. Neurons can have a threshold so that they only send a signal when the total signal exceeds the threshold. Generally, neurons are clustered into layers, and different layers can perform different transformations on their inputs. Signal propagation from the first layer (input layer) to the last layer (output layer) may require multiple traversal of all layers.

For system modeling, the main feature of an artificial neural network is that it has strong adaptability and capacity in the process of dealing with actual problems. In the actual modeling process, there is no need to know the composition of the research object, but only need to limit the topology of the neural network. Its weight or threshold not only specifies the parameters of the model, but also specifies the structure and properties of the model. An accurate network model can be obtained by using the known input and output data as learning and testing samples for training.

BP neural network (Back Propagation Neural Network) is a multi-layer feedforward neural network based on the error back propagation algorithm, which consists of two parts: the forward transmission of information and the back propagation of errors [57,58]. In the process of forward propagation, through the training and testing of samples, the input information is calculated layer by layer through the weight or threshold between the input layer to the hidden layer, and the hidden layer to the output layer. Finally, the result is passed to the output layer. If the deviation between the result of the output layer and the actual value is outside the error range, the error change value of the output layer is calculated. Then the error is back propagated, and the error signal is transmitted back along the original connection path through the network, thereby adjusting the weights of the neurons in each layer. The two processes of forward transmission of information and back propagation of error are repeated until the predicted value of the BP neural network can accurately reflect the result of the actual situation. The process is shown in Figure 11.

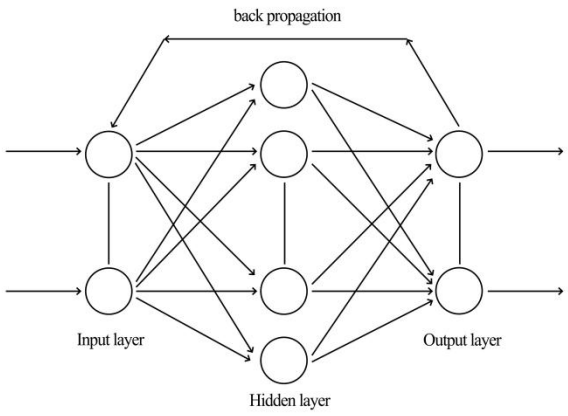

Figure 11. Neural network structure of BP algorithm.

The input neurons of the neural network model established in this paper include design parameters such as the width and depth of different bedrooms and kitchens, as well as the window-to-wall ratios of different rooms and facades. Based on the previous simulation results as the basis of the database, 10,000 sets of data are selected for each city as a sample set to train the prediction model. The output neuron parameters of the model are the annual energy demand per unit area of the building and the annual percentage of UDI 100–2000 lx. According to the output parameters (2) and input parameters (17) of the network model, a three-layer neural network model is established, as shown in Figure 12.

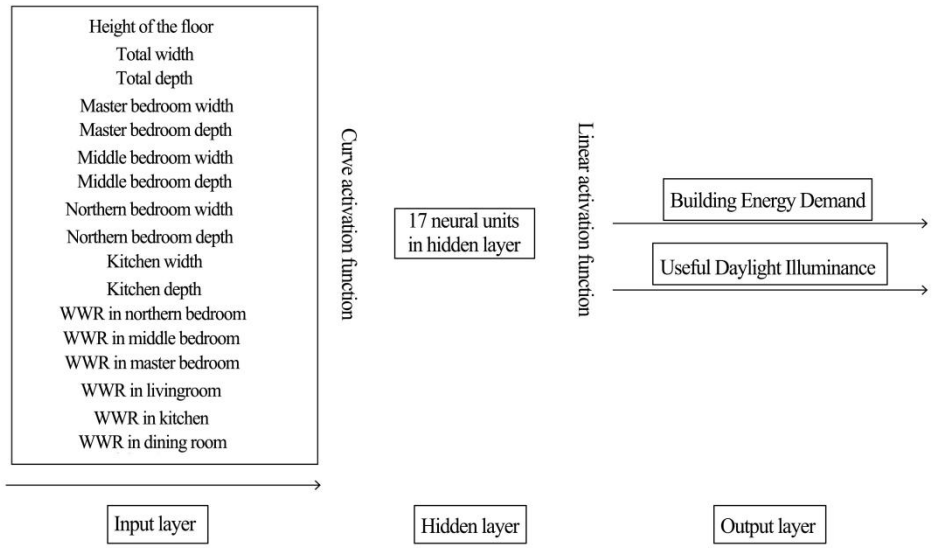

Figure 12. Schematic diagram of BP network model for energy demand and lighting environment comfort of residential buildings.

4.2. Prediction Model Set-Up for Residential Building Simulation in Typical Cities

Taking the climate of Shanghai as an example, 10,000 random simulation data of total energy demand (including heating demand and cooling demand) and annual percentage of Useful Daylight Illuminance (100 lx < UDI < 200 lx) are obtained in the simulation results; the minimum, maximum and average values of the total energy demand per square meter are 71.78 kWh/m^2, 117.40 kWh/m^2 and 94.30 kWh/m^2, respectively. The lowest UDI 100–2000 lx is 38.67% and the highest is 72%. Therefore, through the adjustment of internal space design parameters, the maximum energy-saving rate can reach 38.8% and the maximum light environment improvement rate is 33.4%.

The study did not establish a neural network for each of the typical cities to predict the impact of residential indoor space on energy demand and lighting. Instead, “city" was taken as one of the input data of neural network, and about 10,000 random simulations were conducted for each city. The design parameters used in the Monte Carlo simulation uniformly covered their respective value ranges. Compared with the establishment of different neural network models, this method can greatly reduce the amount of data needed for training neural network under the premise of ensuring the accuracy of prediction, thus saving simulation time. In order to prevent the neural network from over-fitting, the cross validation method is used to divide the training set and test set according to the ratio of 8:2. There are more than 40,000 data in training set and more than 10,000 data in test set. Before training, in order to speed up the convergence of the neural network and improve the accuracy of prediction, the data were normalized in the process of training a neural network model; when indicators such as the root mean square error of the model tend to be stabilized, it can be considered that the model has reached convergence. If the error is small enough, it indicates that the prediction effect of the neural network is good, and it can replace the building simulation as the adaptive

evaluation in the multi-objective optimization. Table 7 shows the performance of the neural network model on the training set and the validation set. The results show that the error of the neural network has been controlled within an acceptable range. In order to visually demonstrate the predictive ability of the neural network model, the study randomly selected 100 data from the test set to compare with the prediction results of the neural network. The results are shown in Appendix Figures A1–A4.

Table 7. Fitting index of neural network prediction model.

Data Set	Data Type	MAE	MSE	R^2
Training set	Cooling demand	0.067	0.012	1.000
	Heating demand	0.056	0.007	1.000
	Light environment (UDI index)	0.261	0.207	0.996
Test set	Cooling demand	0.072	0.009	1.000
	Heating demand	0.059	0.006	1.000
	Light environment (UDI index)	0.318	0.304	0.994

4.3. Sensitivity Analysis of Design Parameters of Residential Interior Space

The study is based on 15,000 sets of data obtained for each city in a Monte Carlo simulation, and uses IBM SPSS Statistics 24 to analyze the Spearman correlation coefficient between the parameters and the objective function. The correlation analysis results are shown in Appendix Tables A1–A5. In regard to the Spearman correlation coefficient, the coefficient has high correlation in the range 0.8–1, strong correlation in the range 0.6–0.8, medium correlation in the range 0.4–0.6, weak correlation in the range 0.2–0.4 and extremely weak correlation in the range 0–0.2 [59].

It can be seen from Tables A1–A5 that the depth and width variables of each room have a moderate impact on the Useful Daylight Illuminance (UDI 100–2000 lx), because the Spearman coefficient of the relevant design parameters is between 0.3 and 0.5. Compared with these parameters, the window-to-wall ratio of each room has a weaker influence on the lighting environment, with the Spearman coefficient in between 0.1 and 0.3. Regarding the total energy demand, floor height has a strong influence on it for each typical city. However, except for the climatic conditions of Shenzhen and Kunming where the depth and width of each room have a moderate impact, under the climatic conditions of Harbin, Beijing and Shanghai, the depth and width of each room have a weak influence on it (generally less than 0.3). Except for Kunming, under the climatic conditions of Harbin, Beijing and Shanghai, the influence of room depth and width on building cooling demand is significantly higher than that on heating demand. In Kunming, these design parameters have similar effects on cooling and heating; while in Shenzhen, since there is no heating time period, the influence of design parameters on heating demand is zero. In addition, under the climatic conditions of typical cities, the window-to-wall ratio of each room has a higher impact on building cooling demand than it has on building heating demand.

In addition to the analysis of Spearman coefficient, the study also conducted a local sensitivity analysis of different design parameters to understand the influence of each design parameter on the objective function under different climate conditions. However, due to the large number of design parameters, and each of them affects more than one objective function, Figures 13–28 only select 4 typical design parameters for local sensitivity analysis, namely floor height, total width, master bedroom window-to-wall ratio and living room window-to-wall ratio to intuitively understand the changes of objectives under different climatic conditions.

From Figures 13–15, it can be seen that with the increase in floor height, the total energy demand for residential buildings in each city is increasing, where the increase in Harbin climate is the largest and the energy demand per unit building area is much higher

than that of other cities, while the increase in Kunming is the smallest. The heating and cooling demand of different cities account for different proportions of the total energy demand. The energy demand in Harbin mainly comes from heating which is about 160–205 kWh/m^2, while the cooling demand is only 5–10 kWh/m^2. Under the climatic conditions of Beijing and Shanghai, the heating demand is higher than the cooling demand. The heating demand is about 50–110 kWh/m^2, while the cooling demand is only 15–35 kWh/m^2. Residential buildings under the climate conditions in Shenzhen are different from the above cities where the building energy demand comes only from the cooling demand, which is about 65–85 kWh/m^2. In addition, compared with other cities, residential heating and cooling demand under the climatic conditions of Kunming are at a lower value, indicating the climate there is quite pleasant.

From the analysis of lighting environment and floor height in Figure 16, it can be seen that with the increase of floor height, under all typical climate conditions, the annual percentage of UDI 100 lx–2000 lx is decreasing. By comparing the residential indoor light environment in different cities, it is clear to see that Kunming has the best indoor light environment, followed by Shenzhen, Beijing and Shanghai, and Harbin has the worst indoor light environment, resulting from different latitude and solar angles in different cities. Through the sensitivity analysis of the floor height, it can be summarized that with the increase of the floor height, the energy demand and the indoor lighting environment are deteriorating. Therefore, it is recommended to control the floor height at 2.7 m in order to obtaining the optimal goals.

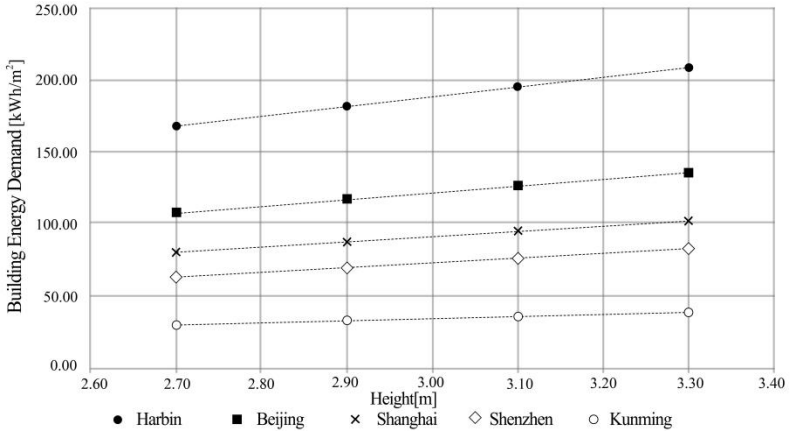

Figure 13. Relationship between building total energy demand and floor height.

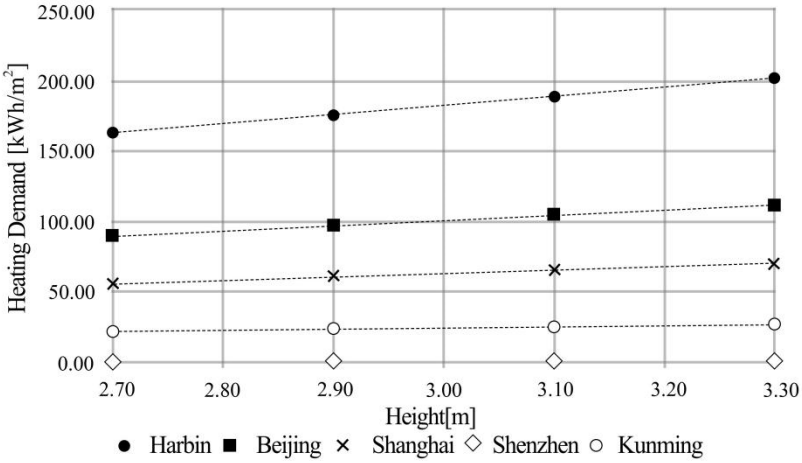

Figure 14. Relationship between heating demand and floor height.

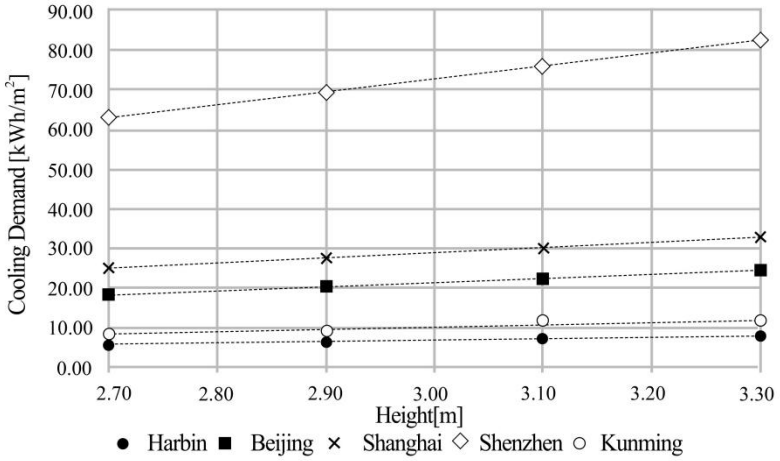

Figure 15. Relationship between cooling demand and floor height.

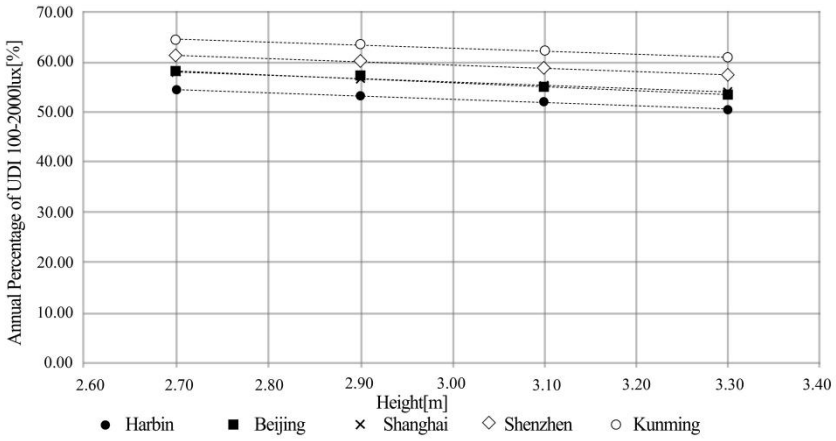

Figure 16. The relationship between annual percentage of UDI 100–2000 lx and floor height.

Since the total area of the apartment is always controlled at 118 m², the total width and the total depth are symmetrical with respect to the objective function. Therefore, the study only conducts local sensitivity analysis for the total width of the apartment. Figures 17–19 show the relationship of the total width and the building energy demand, where it is clear to see that the total energy demand under the climate conditions of Harbin and Beijing gradually decreases as the total width increases, while under Shanghai climate conditions, the total width has little influence on the fluctuation of total energy demand. Moreover, under the climatic conditions of Shenzhen and Kunming, as the total width increases, the total energy demand is gradually increasing. This is because in residential buildings in Harbin and Beijing, as the total width becomes larger, the heating demand is decreasing. Although the corresponding cooling demand increases slightly, the magnitude is not as large as the change in heating demand, which leads to a decrease in total energy demand. Specifically, under the climate conditions of Harbin, the total energy demand decreases from 235 kWh/m² to about 200 kWh/m² as the width increases, and under Beijing climatic conditions, the total energy demand decreases from 150 kWh/m² to about 135 kWh/m² as the width increases. Different to Harbin and Beijing, the total energy demand of residential buildings in Shenzhen and Kunming has increased with the increase in width, mainly because the change in heating demand is relatively stable, while the demand for cooling has increased. For example, under the climatic conditions in Shenzhen, as the width of the house becomes larger, the cooling demand has increased from 80 kWh/m² to about 90 kWh/m².

According to the analysis of the total width and the annual percentage of UDI 100 lx–2000 lx in Figure 20, as the width increases, the annual percentage of UDI100 lx–2000 lx is decreasing. Among them, Kunming has the best indoor light environment, followed by Shenzhen, Shanghai and Beijing. Harbin's indoor light environment comfort is worse than other cities.

Through the sensitivity analysis of the total width, it can be seen that under different typical urban climate conditions, the change in the total width of the house has different correlations with the objective function. The main difference lies in the impact on the total energy demand. Therefore, it is necessary to perform an optimization search on a global scale to find the optimal width value that weighs the total energy demand and the comfort of the light environment.

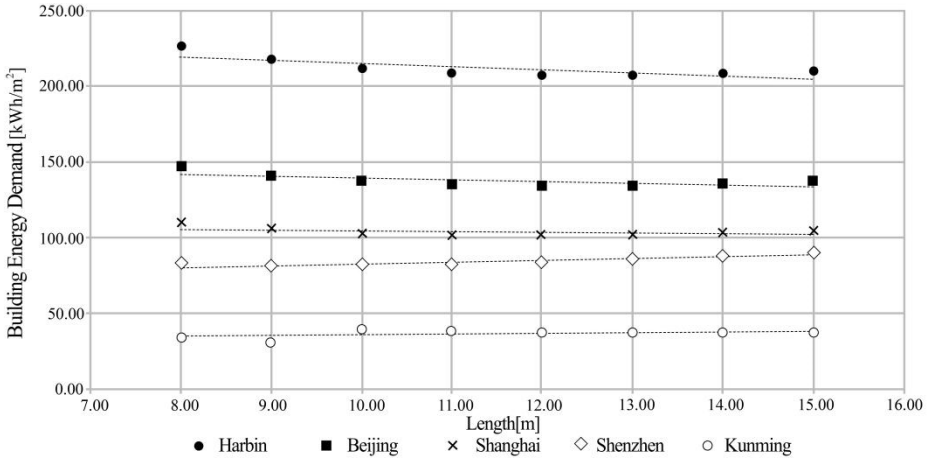

Figure 17. Relationship between building total energy demand and total width.

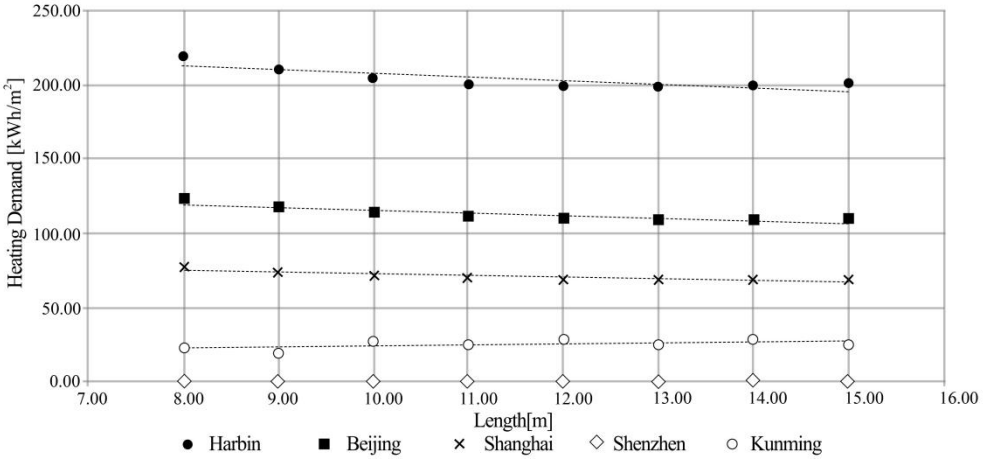

Figure 18. Relationship between heating demand and total width.

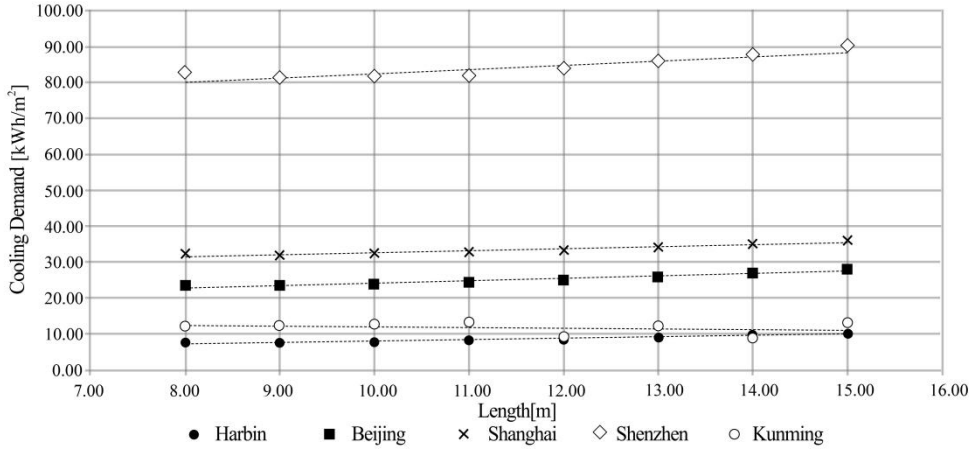

Figure 19. Relationship between cooling demand and total width.

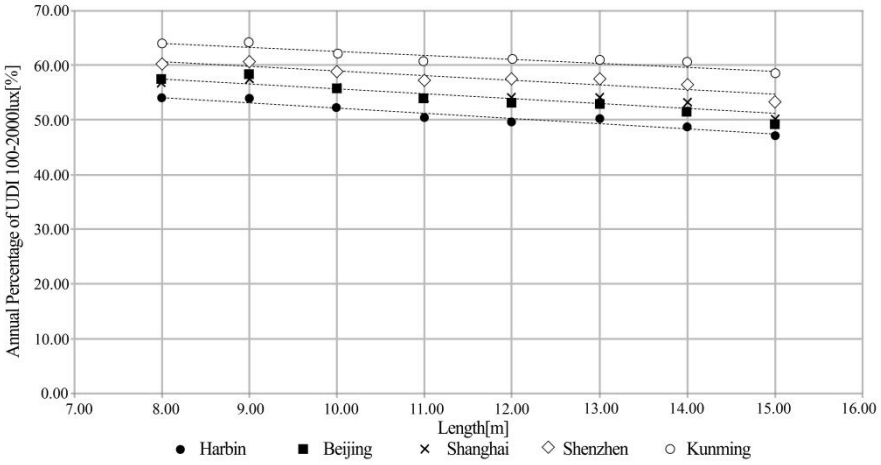

Figure 20. The relationship between annual percentage of UDI 100–2000 lx and total width.

Figures 21–23 analyze the effect of the window-to-wall ratio of the master bedroom on the total energy demand (including heating demand and cooling demand) and annual percentage of UDI 100–2000 lx. It can be seen that the increase in the window-to-wall ratio of the master bedroom has little effect on the total energy demand of residential buildings in cities other than Shenzhen where the total energy demand of residential buildings has increased. This is because the increase in window area has led to a significant increase in the demand for cooling in the area, from 82 kWh/m² to 95 kWh/m². From the analysis in Figure 24, it can be seen that with the increase in the window-to-wall ratio in the master bedroom, annual percentage of UDI 100–2000 lx in all typical cities has gradually decreased, thus the lighting environment comfort has a certain degree of degradation.

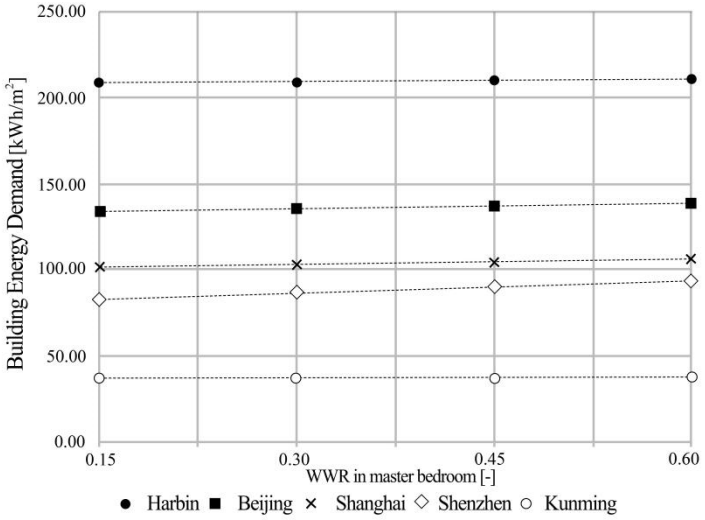

Figure 21. Relationship between building total energy demand and window-to-wall ratio in master bedroom.

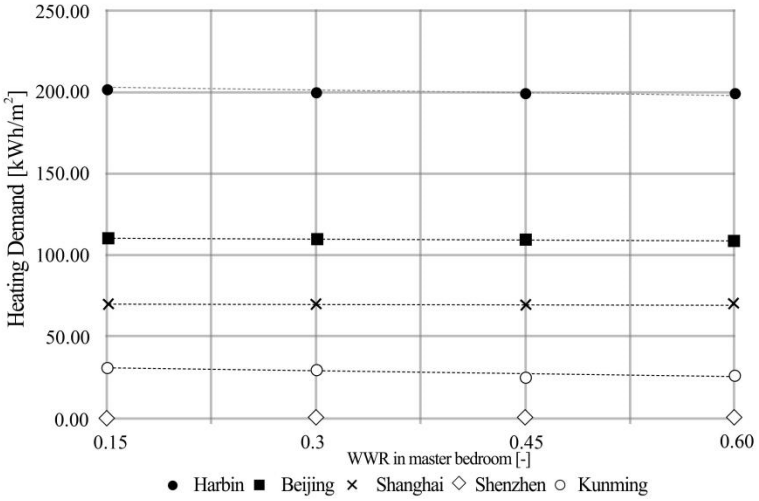

Figure 22. Relationship between building heating demand and window-to-wall ratio in master bedroom.

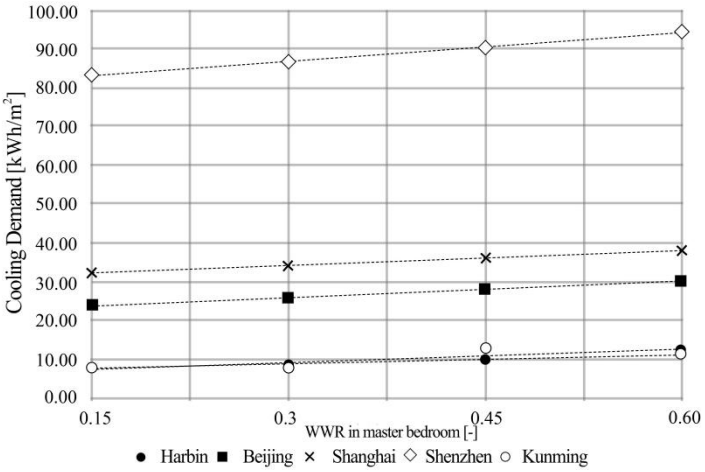

Figure 23. Relationship between building cooling demand and window-to-wall ratio in master bedroom.

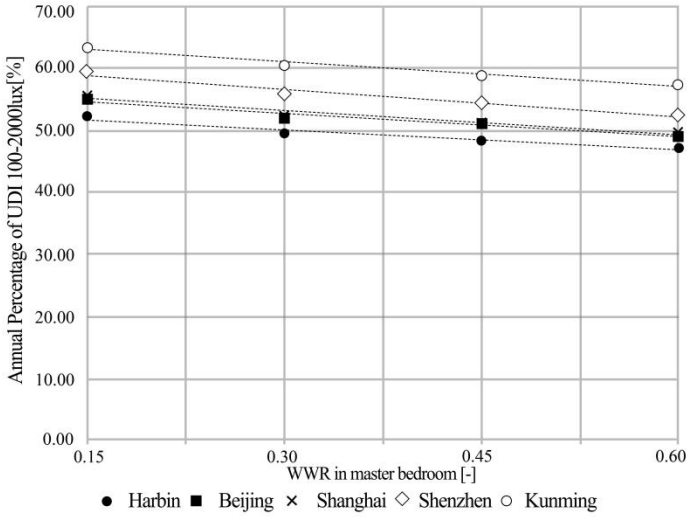

Figure 24. The relationship between annual percentage of UDI 100–2000 lx and window-to-wall ratio in master bedroom.

Figures 25–27 analyze the impact of window-to-wall ratio in the living room on the total energy demand (including heating demand and cooling demand) and annual percentage of UDI 100–2000 lx. With the increase in the window-to-wall ratio in the living room, the total energy demand of residential buildings under the climate of Shenzhen is also increasing, but that under the climatic conditions of Kunming is decreasing, and there is little fluctuation in other cities. This is because with the increase in the window-to-wall ratio in the living room, more solar radiation enters the room, leading to a significant increase in residential cooling demand in Shenzhen, from 210 kWh/m^2 to about 240 kWh/m^2. However, due to different climatic conditions, the demand for residential cooling in Kunming has slightly decreased, from 30 kWh/m^2 to about 20 kWh/m^2.

From the analysis in Figure 28 which shows the impact of the window-to-wall ratio in the living room on the indoor lighting environment, it is summarized that with the window-to-wall ratio increases, the annual percentage of UDI 100–2000 lx in each typical city gradually decreases, therefore, the light environment comfort has a certain degree of degradation.

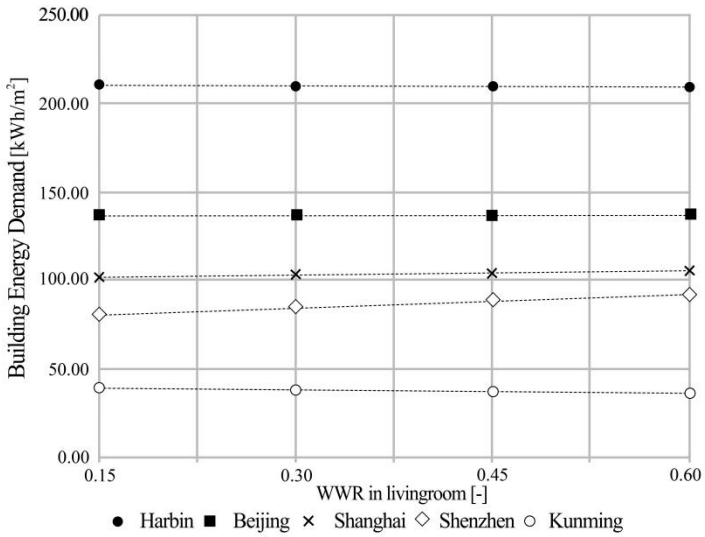

Figure 25. Relationship between building total energy demand and window-to-wall ratio in living room.

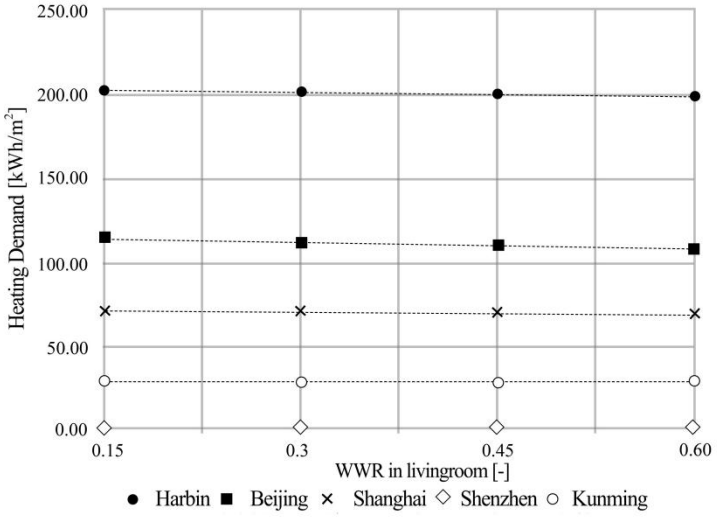

Figure 26. Relationship between building heating demand and window-to-wall ratio in living room.

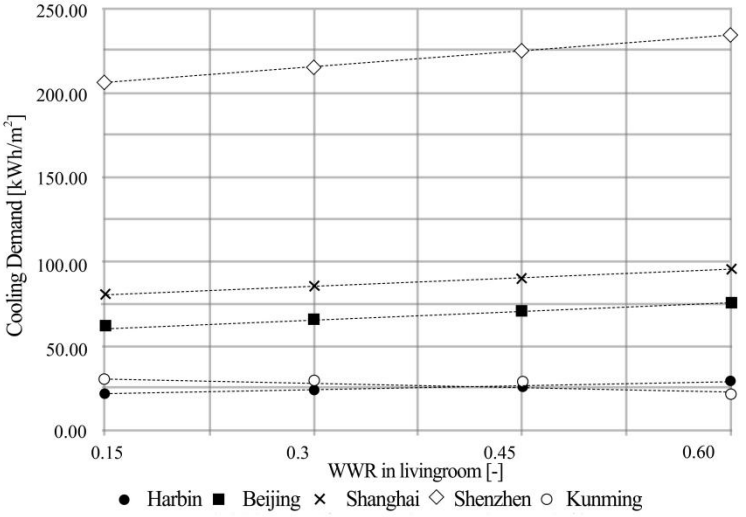

Figure 27. Relationship between building cooling demand and window-to-wall ratio in living room.

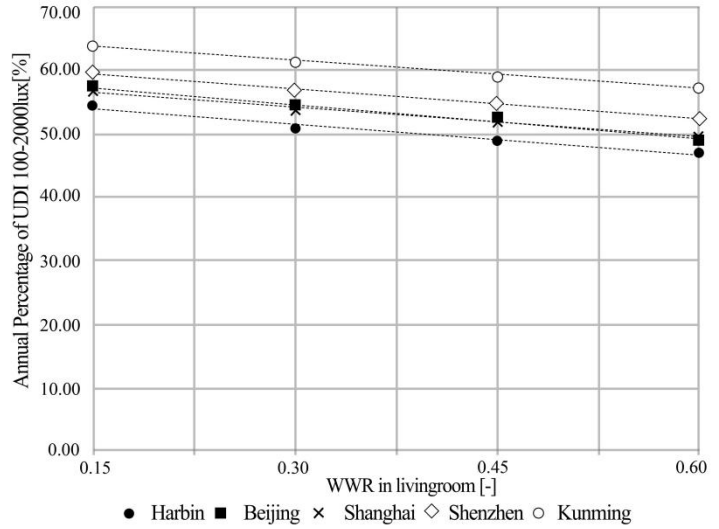

Figure 28. Relationship between annual percentage of UDI 100–2000 lx and window-to-wall ratio in living room.

5. Discussion of Optimization Results

5.1. Optimization Results of Residential Interior Design in Typical Cities

The research obtained the best solution through parametric performance simulation and NSGA-II algorithm to optimize all design parameters, as shown in Figure 29, where the darkest part in red is the Pareto front. Tables 8 and 9 list the best building energy demand (that is, the smallest building energy demand solution, nZEB optimal solution) and the best light environment (that is, the highest annual percentage of UDI 100 lx–2000 lx, UDI optimal solution) for each city under different climatic conditions and its corresponding design parameters.

It can be seen from Table 8 that in the optimal design of nZEB and UDI in all cities, the floor height is 2.7 m. Furthermore, in nZEB solution, the total depth and total width of residential buildings in Harbin, Beijing and Shenzhen are the same (total width is 14.97 m, total depth is 7.88 m), while those parameters in Shanghai and Kunming are different. The total width in Shanghai nZEB optimal solution is 12.28 m and the total depth is 9.61 m; the total width in Kunming nZEB optimal solution is 11.20 m and the total depth is 10.54 m, leading to the fact that the difference of nZEB optimal design parameters in Harbin, Beijing and Shenzhen are mainly from the difference in depth between the master bedroom and the middle bedroom. With respect of the window-to-wall ratio of each room, the best window-to-wall ratio in the master bedroom and the living room of Beijing nZEB solution (0.41 and 0.59, respectively) is higher than that of Harbin and Shenzhen nZEB solution (0.19 and 0.32 in Harbin, 0.18 and 0.24 in Shenzhen). However, in general, the window-to-wall ratio in colder cities in the north are larger than those in warm cities in the south. This is because residential buildings in northern cities need to introduce more solar radiation into indoor space to reduce heating demand in winter, while southern cities need to reduce the window-to-wall ratio to prevent too much solar radiation from entering the room, thereby reducing the demand for cooling in summer, however, too large window area will also accelerate the flow of indoor energy to the outdoors and reduce the insulation performance of the building. Therefore, the window-to-wall ratio in severe cold areas such as Harbin should not be too large.

In addition, the total depth and total width in the UDI optimal solution for all cities are approximately the same. The total width is 14.97 m and the total depth is 7.88 m, leading to the depth and width of each room being approximately the same. The main difference between the UDI optimal design solution in each city is the window-to-wall ratio parameter of each room. The window-to-wall ratio of the north bedroom, master bedroom and living room of the UDI optimal design solution in Shanghai is greater than that in other cities, which are 0.26, 0.32 and 0.33, respectively. The kitchen window-to-wall ratio of UDI optimal design solution in Shenzhen is greater than that in other cities, which is 0.59. Moreover, the window-to-wall ratios of dining room in Harbin, Beijing and Shenzhen UDI optimal design solution (0.54, 0.50 and 0.60, respectively) are significantly greater than that in Shanghai and Kunming (0.19 and 0.16, respectively).

From the comparison of the performance indicators of the optimal solution in Table 9, it is obvious to see that the heating demand of residential buildings in Harbin, Beijing and Shanghai is much higher than the cooling demand. Meanwhile, as mentioned above, the heating schedule in Shenzhen is set to zero, thus the building energy demand in Shenzhen is all from cooling demand. Furthermore, through the comparison of the optimal energy demand of nZEB and UDI solution in various cities, it can be seen that the energy demand of residential buildings in Beijing is higher than other cities, which are 110.69 kWh/m^2 and 137.48 kWh/m^2. While Kunming and Shanghai are the lowest. Besides, with the exception of Beijing, the optimal energy demand indicators in nZEB and UDI solution in each city are not much different. Different from the energy demand index, the index of annual percentage of UDI 100–2000 lx in nZEB optimal solution and UDI optimal

solution in Shanghai and Kunming are quite different. The annual percentage of UDI 100–2000 lx of the two optimal solutions in Shanghai differed by 21.35%, while that in Kunming differed by 15.63%.

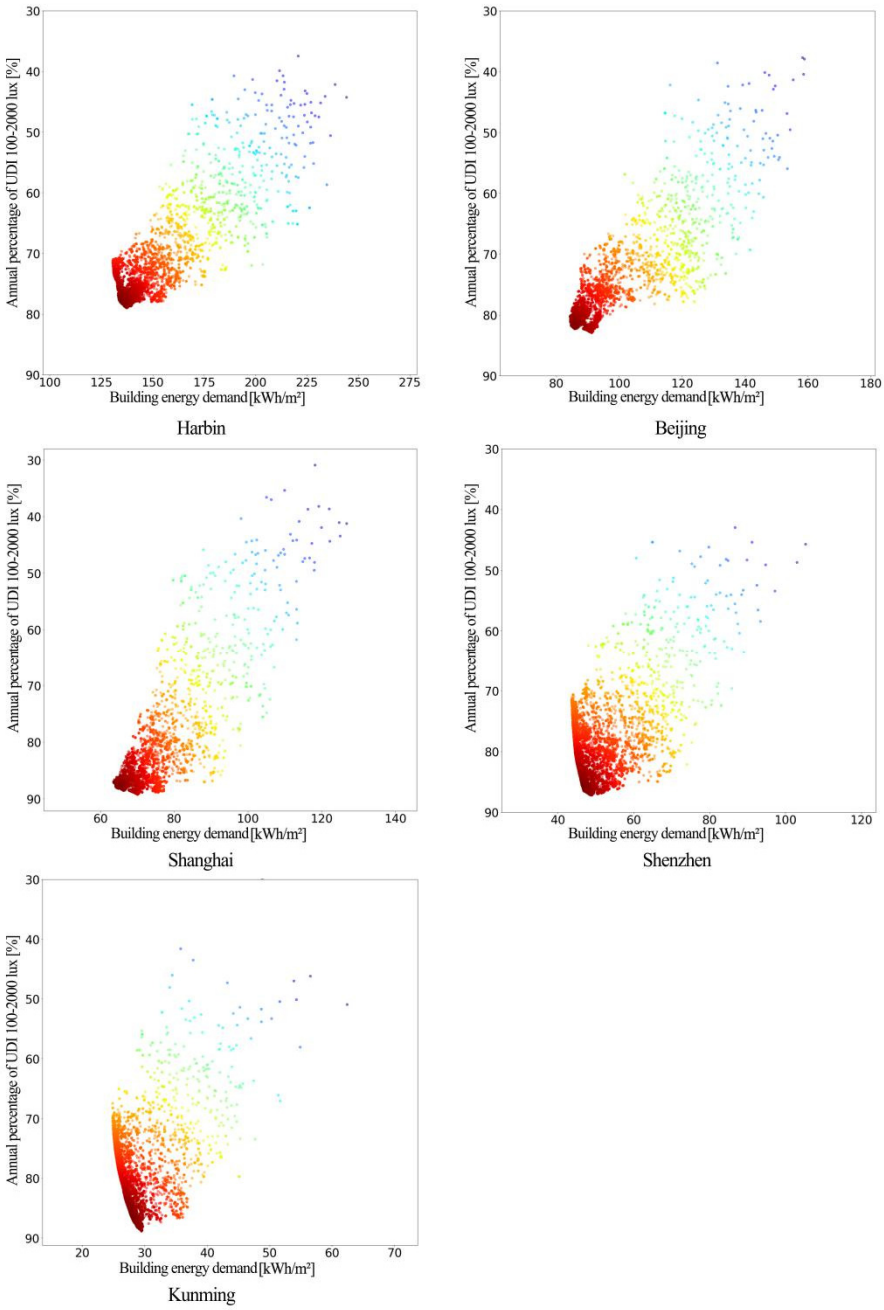

Figure 29. Multi-objective optimization results of typical cities.

Table 8. Optimization design parameters of residential interior space form in typical cities.

Classification	Code	Description	Harbin (Severe Cold Area I)		Beijing (Cold Regions II)		Shanghai (Hot Summer and Cold Winter Area III)		Shenzhen (Hot Summer and Warm Winter Area IV)		Kunming (Temperate Region V)	
			nZEB(*)	UDI(*)	nZEB(*)	UDI(*)	nZEB(*)	UDI(*)	nZEB(*)	UDI(*)	nZEB(*)	UDI(*)
Spatial morphological parameters	A1	Floor height	2.70	2.70	2.70	2.70	2.70	2.70	2.70	2.70	2.70	2.70
	A2	Total width	14.97	14.96	14.97	14.97	12.28	14.98	14.98	14.90	11.20	14.92
	A3	Total depth	7.88	7.89	7.88	7.88	9.61	7.88	7.88	7.92	10.54	7.91
	A4	Master bedroom width	2.50	2.50	2.50	2.50	4.42	2.51	2.50	2.50	3.63	2.50
	A5	Master bedroom depth	3.94	4.48	2.59	4.48	4.58	4.47	4.23	4.42	4.88	4.51
	A6	Middle bedroom width	2.50	2.50	2.50	2.50	4.42	2.51	2.50	2.50	3.63	2.50
	A7	Middle bedroom depth	2.24	1.70	3.60	1.70	3.18	1.70	1.88	1.73	3.89	1.70
	A8	North bedroom width	2.50	2.50	2.50	2.50	4.42	2.51	2.50	2.50	3.63	2.50
	A9	North bedroom depth	1.70	1.71	1.70	1.70	1.85	1.71	1.77	1.77	1.77	1.70
	A10	Kitchen width	1.70	4.95	1.71	1.74	1.96	1.70	1.70	5.00	1.70	1.74
	A11	Kitchen depth	1.70	1.71	1.70	1.70	1.85	1.71	1.77	1.77	1.77	1.70
Window parameters	B1	Window-to-wall ratio in north bedroom	0.15	0.16	0.15	0.27	0.29	0.26	0.15	0.18	0.15	0.15
	B2	Window-to-wall ratio in middle bedroom	0.15	0.15	0.15	0.15	0.15	0.15	0.15	0.15	0.15	0.15
	B3	Window-to-wall ratio in master bedroom	0.19	0.15	0.41	0.15	0.49	0.32	0.18	0.16	0.15	0.36
	B4	Window-to-wall ratio in living room	0.32	0.15	0.59	0.20	0.60	0.33	0.24	0.16	0.15	0.17
	B5	Window-to-wall ratio in Kitchen	0.23	0.28	0.16	0.20	0.24	0.33	0.15	0.59	0.15	0.18
	B6	Window-to-wall ratio in dining room	0.15	0.54	0.15	0.50	0.16	0.19	0.15	0.60	0.15	0.16

nZEB(*): the best solution for annual energy demand, UDI(*): the best solution for the annual percentage of UDI 100–2000 lx.

Table 9. Performance index of optimal solution.

Objective Function	Harbin (Severe Cold Area I)		Beijing (Cold Regions II)		Shanghai (Hot Summer and Cold Winter Area III)		Shenzhen (Hot Summer and Warm Winter Area IV)		Kunming (Temperate Region V)	
	nZEB(*)	UDI(*)	nZEB(*)	UDI(*)	nZEB(*)	UDI(*)	nZEB(*)	UDI(*)	nZEB(*)	UDI(*)
BED (kWh/m²): Building energy demand	84.36	91.23	110.69	137.48	24.86	29.47	63.57	70.08	23.69	28.85
H (kWh/m²): Heating energy demand	70.36	77.46	104.57	132.69	24.77	27.82	0	0	17.05	19.10
C (kWh/m²): Cooling energy demand	14.00	13.77	6.12	4.79	0.09	1.65	63.57	70.08	6.64	9.75
UDI 100–2000 (%): Useful Daylight Illuminance	80.27	82.92	71.43	78.99	67.49	88.84	87.06	89.24	71.56	87.19

nZEB(*): the best solution for annual energy demand, UDI(*): the best solution for the annual percentage of UDI 100–2000 lx.

5.2. Comparison of Optimization Results with Reference Model

Table 10 compares the optimal indicators of each city with the simulated indicators of the reference house. As far as Harbin is concerned, the energy demand of the two optimization results is greatly reduced compared with the reference building, and the main reason for the decrease is that the heating demand is greatly reduced on the basis of a small increase in cooling demand. Heating demand has been reduced by 103.95 kWh/m²

and 96.85 kWh/m² respectively. In addition, in terms of the annual percentage of UDI 100–2000 lx, the two optimal results of Harbin residential building types have also been greatly improved compared with the reference building, increasing by 23.69 and 26.34%, respectively. However, it is worth noting that under Harbin climatic conditions, the performance indicators of the nZEB optimal solution and the UDI optimal solution have little difference for the improvement to the reference building in terms of these two objective functions.

Table 10. The gap between the optimal solution and the performance index of the reference building.

Objective Function	Harbin (Severe Cold Area I)		Beijing (Cold Regions II)		Shanghai (Hot Summer and Cold Winter Area III)		Shenzhen (Hot Summer and Warm Winter Area IV)		Kunming (Temperate Region V)	
	nZEB(*)	UDI(*)	nZEB(*)	UDI(*)	nZEB(*)	UDI(*)	nZEB(*)	UDI(*)	nZEB(*)	UDI(*)
BED (**) (kWh/m²): Building energy demand	95.06	88.19	4.12	−22.67	60.3	55.69	1.63	−4.88	12.41	7.25
H (**) (kWh/m²): Heating energy demand	103.95	96.85	−7.43	−35.55	35.44	32.39	0	0	8.98	6.93
C (**) (kWh/m²): Cooling energy demand	−8.89	−8.66	11.55	12.88	24.86	23.3	1.63	−4.88	3.43	0.1
UDI 100–2000 (**) (%): Useful Daylight Illuminance	−23.69	−26.34	−11.68	−19.24	−6.74	−28.09	−22.39	−24.57	−4.56	−20.19

nZEB(*): the best solution for annual energy demand, UDI(*): the best solution for the annual percentage of UDI 100–2000 lx, (**) A positive value indicates that the proposed solution reduces the performance index, while a negative value indicates an increase.

In cold regions represented by Beijing, the optimal total energy demand of nZEB is reduced by 4.12 kWh/m² compared to the reference house. The main reason is that the cooling demand decreases more than the increase in heating demand. Meanwhile, the nZEB optimal solution also increases annual percentage of UDI 100–2000 lx 11.68%. Whereas, although an annual percentage of UDI 100–2000 lx is better in the UDI optimal solution which is 19.24% than that in nZEB optimal solution, it increases the total energy demand by 22.67 kWh/m² where cooling demand decreases by 12.88 kWh/m², but the heating demand increases by 35.55 kWh/m².

In the hot summer and cold winter area represented by Shanghai, the total energy demand of the two optimization solutions has been greatly reduced compared with the reference house, which are 60.3 kWh/m² and 55.69 kWh/m², respectively. However, the UDI optimal solution improves the annual percentage of UDI 100–2000 lx (which is 28.09%) better than nZEB optimal solution (6.74%). Therefore, from a global perspective, the UDI optimal solution is more in line with the improvement of multi-objective performance indicators.

In the hot summer and warm winter area represented by Shenzhen, the total energy demand of the two optimization solutions has little change compared to the reference house. Specifically, the nZEB optimal solution reduces 1.63 kWh/m², while the UDI optimal solution only increases 4.88 kWh/m². Since the heating schedule of the model is not set according to the actual situation, the changes in total energy demand all come from cooling demand. Different from the indicator of energy demand, annual percentage of UDI 100–2000 lx have greatly improved by these two optimal solutions which are 22.39% (nZEB optimal solution) and 24.57% (UDI optimal solution), respectively.

Similar to Shenzhen, in the temperate climate zone represented by Kunming, the total energy demand of the two optimal solutions has little change compared to the reference house, where nZEB optimal solution reduces 12.41 kWh/m² and UDI optimal solution reduces 7.25 kWh/ m². However, the improvement of UDI optimal solution for annual percentage of UDI 100–2000 lx is significantly higher than that of nZEB optimal solution.

Specifically, the annual percentage of UDI 100–2000 lx in nZEB optimal solution is increased by 4.56% compared with the reference house, but improved by 20.19% in UDI optimal solution. Therefore, in the actual project, design parameters in UDI optimal solution are more in line with the improvement of global performance indicators.

6. Conclusions

This research uses the meteorological parameters of 5 typical Chinese cities and takes the 118.11 square meter apartment in Tianjin residential community as an example to carry out the optimization analysis for indoor space design. Finally, the optimal indoor space design parameters are explored from the perspective of lowest building energy demand and highest annual percentage of UDI 100–2000 lx. Meanwhile, the design parameters and performance indicators of each typical city are compared and explained to understand the difference of indoor space design under different climate conditions.

From the analysis results, it can be concluded that in the early stage of the schematic design, the indoor space design optimization can effectively reduce the residential energy demand and improve the indoor lighting environment comfort. According to the optimization results in this case, the total energy demand per square meter and the annual percentage of UDI 100–2000 lx in each optimal solution under different typical cities are generally better than the original reference apartment plan.

Under the climate conditions of Harbin, the design parameters of nZEB optimal solution and UDI optimal solution have greatly improved the performance of the reference apartment. Both design optimization results suggest that the total indoor width is 14.97 m, the total depth is 7.88 m, the window-to-wall ratio of the living room is 0.32 (nZEB optimal solution) or 0.15 (the UDI optimal solution), and the value of the restaurant window-to-wall ratio is 0.15 (nZEB optimal solution) or 0.54 (the UDI optimal solution). Under the climate conditions of Shenzhen, both the nZEB optimal solution and UDI optimal solution greatly improve indoor lighting environment comfort, which are 22.39% (nZEB optimal solution) and 24.57% (UDI optimal solution), respectively. However, they have little difference in the improvement of total energy demand, which are 1.63 kWh/m^2 (nZEB optimal solution) and −4.88 kWh/m^2 (UDI optimal solution), respectively. Under Shanghai climatic conditions, compared with the performance index of nZEB optimal solution, the UDI optimal solution has higher overall benefits. Therefore, the recommended total width is 14.98 m and the total depth is 7.88 m. The window-to-wall ratio of north bedroom, master bedroom and living room are 0.26, 0.32 and 0.33, respectively. Similar to Shanghai, the interior design parameters of residential buildings under Kunming climate conditions are also recommended to take the UDI optimal design solution, which means that the total width is 14.92 m, the total depth is 7.91 m, the window-to-wall ratio of the master bedroom is 0.36, and that of the remaining rooms is between 0.15 and 0.18. Different from Shanghai and Kunming, it is recommended to take nZEB optimal design solution for residential building interior design parameters under Beijing climatic conditions, i.e., the total width is 14.97 m, the total depth is 7.88 m, the window-to-wall ratio of the master bedroom and the living room are 0.41 and 0.59, respectively, and that of the rest of the room is 0.15.

Through the correlation analysis between the design parameters and energy demand and the indoor lighting comfort, the indoor space design parameters have a strong influence on the energy-saving design of residential buildings, so it needs to be differentiated according to the climate characteristics of different typical cities, which enables architects to make wise decisions on parameter values according to different climatic conditions, and to meet multiple design intents in terms of architectural function, aesthetics and architectural performance.

Based on the Grasshopper, a parametric multi-objective optimization process was created in this research for the preliminary stage of residential building design. Through sensitivity analysis, the research discusses the relationship between residential indoor space design parameters, building performance and lighting environment, which enables

architects to make design decisions based on parameter sensitivity. The research is only optimized for a specific case, but this method has a certain general applicability and can be widely used in the optimization of different residential interior designs. Therefore, the application and promotion of this optimization method is of great significance to residential projects.

Author Contributions: In this paper, Z.L. performed the experiment, including conceptualization, methodology, writing. Y.Z. performed data visualization. M.T. reviewed and edited it. Y.Y. validated it. All authors organized the paper structure. All authors have read and agreed to the published version of the manuscript.

Funding: This research was funded by Humanities and Social Sciences Fund of Zhejiang Education Department, grant number Y202146952 and Zhejiang University of Technology Liberal Arts Laboratory, Database Construction Project "Zhejiang Historical and Cultural Villages and Towns Spatial Humanities Database", grant number GZ21681180011.

Informed Consent Statement: Informed consent was obtained from all subjects involved in the study.

Data Availability Statement: The data presented in this study are available on request from the corresponding author.

Acknowledgments: The author gratefully acknowledges the editors and referees for their positive and constructive comments in the review process.

Conflicts of Interest: The authors declare no conflicts of interest.

Appendix A

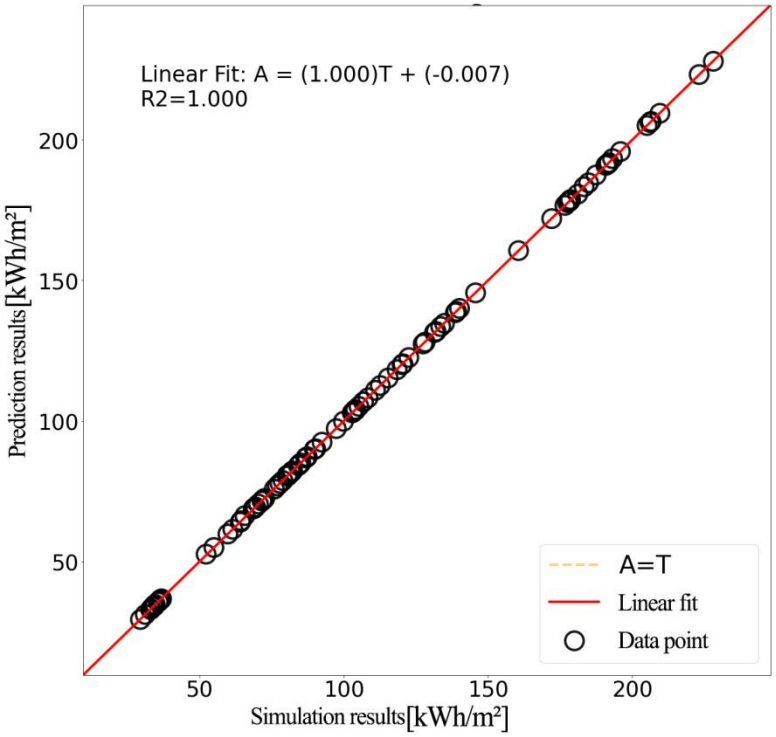

Figure A1. Prediction model of building energy demand.

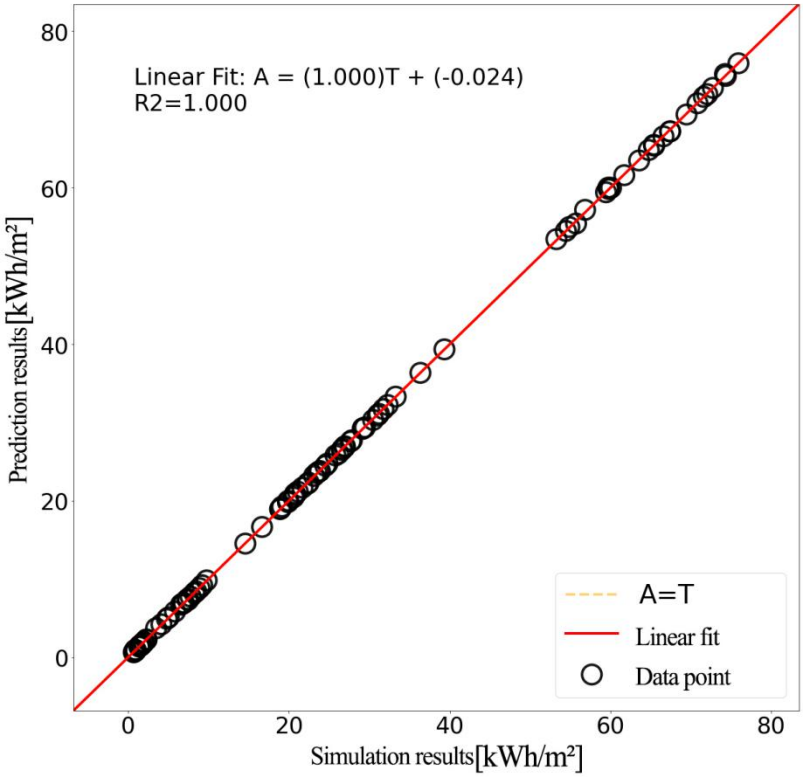

Figure A2. Prediction model of building cooling demand.

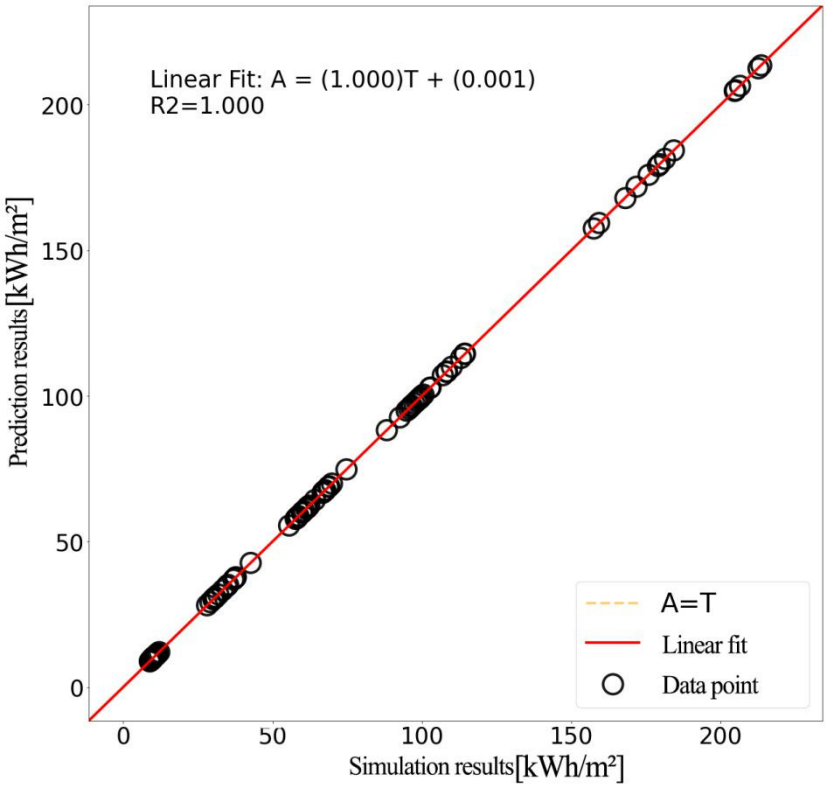

Figure A3. Prediction model of building heating demand.

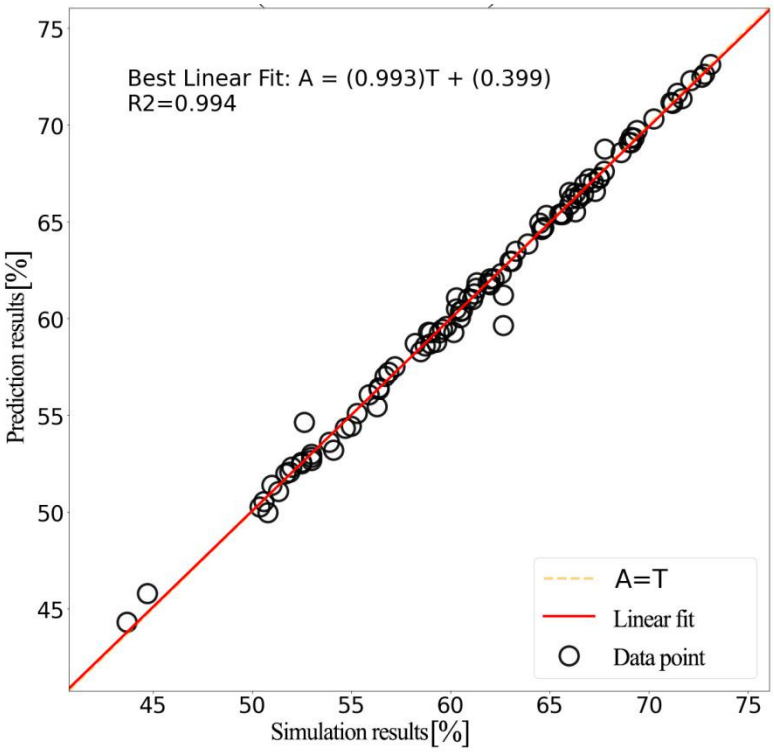

Figure A4. Prediction model of annual percentage of UDI 100–2000 lx.

Table A1. Comparison of Spearman **coefficients** of residential interior space design parameters in Harbin.

Classification	Code	Description	Harbin (Severe Cold Area I)							
			H		C		BED		UDI	
			C*	S*	C*	S*	C*	S*	C*	S*
Spatial morphological parameters	A1	Floor height	0.891	0.00	0.397	0.00	0.898	0.00	0.237	0.00
	A2	Total width	−0.127	0.00	0.523	0.00	−0.062	0.00	−0.579	0.00
	A3	Total depth	0.127	0.00	0.523	0.00	0.062	0.00	0.579	0.00
	A4	Master bedroom width	0.127	0.00	0.523	0.00	0.062	0.00	0.579	0.00
	A5	Master bedroom depth	−0.031	0.00	−0.467	0.00	−0.086	0.00	0.563	0.00
	A6	Middle bedroom width	−0.127	0.00	0.523	0.00	−0.062	0.00	−0.579	0.00
	A7	Middle bedroom depth	−0.129	0.00	−0.258	0.00	−0.155	0.00	0.148	0.00
	A8	North bedroom width	−0.127	0.00	0.523	0.00	−0.062	0.00	0.579	0.00
	A9	North bedroom depth	0.350	0.00	−0.288	0.00	0.307	0.00	0.387	0.00
	A10	Kitchen width	0.049	0.00	0.316	0.00	0.085	0.00	−0.344	0.00
	A11	Kitchen depth	0.350	0.00	−0.288	0.00	0.307	0.00	0.387	0.00
Window parameters	B1	Window-to-wall ratio in north bedroom	0.065	0.00	0.177	0.00	0.084	0.00	−0.124	0.00
	B2	Window-to-wall ratio in middle bedroom	0.028	0.00	0.288	0.00	0.061	0.00	−0.159	0.00
	B3	Window-to-wall ratio in master bedroom	−0.036	0.00	0.437	0.00	0.018	0.00	−0.292	0.00
	B4	Window-to-wall ratio in living room	−0.054	0.00	0.409	0.00	−0.003	0.00	−0.405	0.00
	B5	Window-to-wall ratio in kitchen	0.044	0.00	0.147	0.00	0.060	0.00	−0.102	0.00
	B6	Window-to-wall ratio in dining room	0.034	0.00	0.074	0.00	0.042	0.00	−0.070	0.00

C* coefficient; S* Significance.

Table A2. Comparison of Spearman **coefficients** of residential interior space design parameters in Beijing.

Classification	Code	Description	Beijing (Cold Regions II)							
			H		C		BED		UDI	
			C*	S*	C*	S*	C*	S*	C*	S*
Spatial morphological parameters	A1	Floor height	0.865	0.00	0.522	0.00	0.894	0.00	−0.257	0.00
	A2	Total width	−0.196	0.00	0.472	0.00	0.001	0.00	−0.588	0.00
	A3	Total depth	0.196	0.00	−0.472	0.00	−0.001	0.00	0.588	0.00
	A4	Master bedroom width	−0.196	0.00	0.472	0.00	0.001	0.00	−0.588	0.00
	A5	Master bedroom depth	0.024	0.00	−0.439	0.00	−0.140	0.00	0.502	0.00
	A6	Middle bedroom width	−0.196	0.00	0.472	0.00	0.001	0.00	−0.588	0.00
	A7	Middle bedroom depth	−0.094	0.00	−0.263	0.00	−0.175	0.00	0.087	0.00
	A8	North bedroom width	−0.196	0.00	0.472	0.00	0.001	0.00	−0.588	0.00
	A9	North bedroom depth	0.397	0.00	−0.221	0.00	0.263	0.00	0.510	0.00
	A10	Kitchen width	0.002	0.00	0.293	0.00	0.108	0.00	−0.349	0.00
	A11	Kitchen depth	0.397	0.00	−0.221	0.00	0.263	0.00	0.510	0.00
Window parameters	B1	Window-to-wall ratio in north bedroom	0.055	0.00	0.188	0.00	0.118	0.00	−0.168	0.00
	B2	Window-to-wall ratio in middle bedroom	0.009	0.00	0.264	0.00	0.103	0.00	−0.172	0.00
	B3	Window-to-wall ratio in master bedroom	−0.075	0.00	0.389	0.00	0.078	0.00	−0.292	0.00
	B4	Window-to-wall ratio in living room	−0.157	0.00	0.397	0.00	0.012	0.00	−0.358	0.00
	B5	Window-to-wall ratio in kitchen	0.028	0.00	0.146	0.00	0.079	0.00	−0.132	0.00
	B6	Window-to-wall ratio in dining room	0.036	0.00	0.084	0.00	0.063	0.00	−0.103	0.00

C* coefficient; S* Significance.

Table A3. Comparison of Spearman **coefficients** of residential interior space design parameters in Shanghai.

Classification	Code	Description	Shanghai (Hot Summer and Cold Winter Area III)							
			H		C		BED		UDI	
			C*	S*	C*	S*	C*	S*	C*	S*
Spatial morphological parameters	A1	Floor height	0.879	0.00	0.645	0.00	0.894	0.00	−0.21	0.00
	A2	Total width	−0.172	0.00	0.396	0.00	0.078	0.00	−0.599	0.00
	A3	Total depth	0.172	0.00	−0.396	0.00	−0.078	0.00	0.599	0.00
	A4	Master bedroom width	−0.172	0.00	0.396	0.00	0.078	0.00	0.599	0.00
	A5	Master bedroom depth	0.008	0.00	−0.388	0.00	−0.188	0.00	0.455	0.00
	A6	Middle bedroom width	−0.172	0.00	0.396	0.00	0.078	0.00	−0.599	0.00
	A7	Middle bedroom depth	−0.118	0.00	−0.242	0.00	−0.196	0.00	0.274	0.00
	A8	North bedroom width	−0.172	0.00	0.396	0.00	0.078	0.00	−0.599	0.00
	A9	North bedroom depth	0.387	0.00	−0.148	0.00	0.190	0.00	0.405	0.00
	A10	Kitchen width	0.029	0.00	0.256	0.00	0.146	0.00	−0.338	0.00
	A11	Kitchen depth	0.387	0.00	−0.148	0.00	0.190	0.00	0.405	0.00
Window parameters	B1	Window-to-wall ratio in north bedroom	0.035	0.00	0.198	0.00	0.123	0.00	−0.063	0.00
	B2	Window-to-wall ratio in middle bedroom	0.012	0.00	0.244	0.00	0.130	0.00	−0.107	0.00
	B3	Window-to-wall ratio in master bedroom	−0.061	0.00	0.330	0.00	0.125	0.00	−0.331	0.00
	B4	Window-to-wall ratio in living room	0.357	0.00	−0.113	0.00	0.102	0.00	−0.435	0.00
	B5	Window-to-wall ratio in kitchen	0.006	0.00	0.155	0.00	0.083	0.00	−0.006	0.00
	B6	Window-to-wall ratio in dining room	0.025	0.00	0.086	0.00	0.062	0.00	0.026	0.00

C* coefficient; S* Significance.

Table A4. Comparison of **Spearman** coefficients of residential interior space design parameters in Shenzhen.

Classification	Code	Description	Shenzhen (Hot Summer and Warm Winter Area IV)							
			H		C		BED		UDI	
			C*	S*	C*	S*	C*	S*	C*	S*
Spatial morphological parameters	A1	Floor height	0.00	0.00	0.733	0.00	0.733	0.00	−0.239	0.00
	A2	Total width	0.00	0.00	0.350	0.00	0.350	0.00	−0.589	0.00
	A3	Total depth	0.00	0.00	−0.350	0.00	−0.350	0.00	0.589	0.00
	A4	Master bedroom width	0.00	0.00	0.350	0.00	0.350	0.00	−0.589	0.00
	A5	Master bedroom depth	0.00	0.00	−0.369	0.00	−0.369	0.00	0.429	0.00
	A6	Middle bedroom width	0.00	0.00	0.350	0.00	0.350	0.00	−0.589	0.00
	A7	Middle bedroom depth	0.00	0.00	−0.253	0.00	−0.253	0.00	0.023	0.00
	A8	North bedroom width	0.00	0.00	0.350	0.00	0.350	0.00	−0.589	0.00
	A9	North bedroom depth	0.00	0.00	−0.077	0.00	−0.077	0.00	0.633	0.00
	A10	Kitchen width	0.00	0.00	0.244	0.00	0.244	0.00	−0.347	0.00
	A11	Kitchen depth	0.00	0.00	−0.077	0.00	−0.077	0.00	0.633	0.00
Window parameters	B1	Window-to-wall ratio in north bedroom	0.00	0.00	0.181	0.00	0.181	0.00	−0.191	0.00
	B2	Window-to-wall ratio in middle bedroom	0.00	0.00	0.186	0.00	0.186	0.00	−0.161	0.00
	B3	Window-to-wall ratio in master bedroom	0.00	0.00	0.282	0.00	0.282	0.00	−0.236	0.00
	B4	Window-to-wall ratio in living room	0.00	0.00	0.308	0.00	0.308	0.00	−0.271	0.00
	B5	Window-to-wall ratio in kitchen	0.00	0.00	0.132	0.00	0.132	0.00	−0.165	0.00
	B6	Window-to-wall ratio in dining room	0.97	0.97	0.097	0.00	0.097	0.00	−0.126	0.00

C* coefficient; S* Significance.

Table A5. Comparison of Spearman coefficients of residential interior space design parameters in Kunming.

Classification	Code	Description	Kunming (Temperate Region V)							
			H		C		BED		UDI	
			C*	S*	C*	S*	C*	S*	C*	S*
Spatial morphological parameters	A1	Floor height	0.808	0.00	0.278	0.00	0.838	0.00	−0.238	0.00
	A2	Total width	−0.236	0.00	0.289	0.00	−0.182	0.00	−0.599	0.00
	A3	Total depth	0.236	0.00	−0.289	0.00	0.182	0.00	0.599	0.00
	A4	Master bedroom width	−0.236	0.00	0.289	0.00	−0.182	0.00	−0.599	0.00
	A5	Master bedroom depth	0.044	0.00	−0.286	0.00	−0.007	0.00	0.489	0.00
	A6	Middle bedroom width	−0.236	0.00	0.289	0.00	−0.182	0.00	−0.599	0.00
	A7	Middle bedroom depth	−0.097	0.00	−0.036	0.00	−0.101	0.00	0.054	0.00
	A8	North bedroom width	−0.236	0.00	0.289	0.00	−0.182	0.00	−0.599	0.00
	A9	North bedroom depth	0.449	0.00	−0.209	0.00	0.406	0.00	0.568	0.00
	A10	Kitchen width	−0.012	0.00	0.179	0.00	0.020	0.00	−0.362	0.00
	A11	Kitchen depth	0.449	0.00	−0.209	0.00	0.406	0.00	0.568	0.00
Window parameters	B1	Window-to-wall ratio in north bedroom	0.029	0.00	0.137	0.00	0.052	0.00	−0.169	0.00
	B2	Window-to-wall ratio in middle bedroom	−0.023	0.00	0.601	0.00	0.069	0.00	−0.161	0.00
	B3	Window-to-wall ratio in master bedroom	−0.101	0.00	0.457	0.00	−0.023	0.00	−0.257	0.00
	B4	Window-to-wall ratio in living room	−0.248	0.00	0.162	0.00	−0.215	0.00	−0.278	0.00
	B5	Window-to-wall ratio in kitchen	0.003	0.00	0.125	0.00	0.025	0.00	−0.137	0.00

	B6	Window-to-wall ratio in dining room	0.018	0.00	0.032	0.00	0.024	0.00	−0.100	0.00

C* coefficient; S* Significance.

References

1. U.S. Energy Information Administration. *Annual Energy Outlook 2014*; US Department of Energy: Washington, DC, USA, 2014; Volume 0383, pp. 1–269.
2. Guo, S.; Yan, D.; Hu, S.; Zhang, Y. Modelling building energy consumption in China under different future scenarios. *Energy* **2021**, *214*, 119063.
3. Kylili, A.; Fokaides, P.A.; Jimenez, P.A.L. Key Performance Indicators (KPIs) approach in buildings renovation for the sustainability of the built environment: A review. *Renew. Sustain. Energy Rev*. **2016**, *56*, 906–915.
4. Xu, W.; Liu, Z.; Chen, X.; Zhang, S.C. Thoughts of development of Chinese nearly zero energy buildings. *Build. Sci.* **2016**, *32*, 1–5.
5. UN General Assembly. *Transforming Our World: The 2030 Agenda for Sustainable Development*; A/RES/70/1; UN General Assembly: New York, NY, USA, 2015.
6. D'Agostino, D. Assessment of the progress towards the establishment of definitions of Nearly Zero Energy Buildings (nZEBs) in European Member States. *J. Build. Eng.* **2015**, *1*, 20–32.
7. Teitelbaum, E.; Jayathissa, P.; Miller, C. Forrest Meggers, Design with Comfort: Expanding the psychrometric chart with radiation and convection dimensions. *Energy Build.* **2020**, *209*, 109591.
8. Olgyay, V. *Design with Climate, Bioclimatic Approach to Architectural Regionalism*; Princeton University Press: Princeton, NJ, USA, 1963; p. 125.
9. Givoni, B. *Man, Climate and Architecture*; Applied Science Publisher: London, UK, 1969.
10. Alsousi, M. User Response to Energy Conservation and Thermal Comfort of High-Rise Residential Buildings in Hot Humid Region with Referring to Gaza. Ph.D. Thesis, University of Nottingham, Nottingham, UK, 2005.
11. Ghisi, E.; Massignani, R.F. Thermal performance of bedrooms in a multi-storey residential building in southern Brazil. *Build. Environ.* **2007**, *42*, 730–742.
12. Schnieders, J.; Feist, W.; Rongen, L. Passive Houses for different climate zones. *Energy Build.* **2015**, *105*, 71–87.
13. Martinelli, L.; Matzarakis, A. Influence of height/width proportions on the thermal comfort of courtyard typology for Italian climate zones. *Sustain. Cities Soc.* **2017**, *29*, 97–106.
14. Harkouss, F.; Fardoun, F.; Biwole, P. Passive design optimization of low energy buildings in different climates. *Energy*, **2018**, *165*, 591–613.
15. Harkouss, F. Optimal Design of Net Zero Energy Buildings under Different Climates. Ph.D. Thesis, Université Côte d'Azur, Provence, France, Université Libanaise, Beirut, Lebanon, 2018.
16. Ascione, F.; Bianco, N.; Mauro, G.M.; Napolitano, D.F. Building envelope design: Multi-objective optimization to minimize energy consumption, global cost and thermal discomfort. Application to different Italian climatic zones. *Energy* **2019**, *174*, 359–374.
17. Coma, J.; Maldonado, J.M.; de Gracia, A.; Gimbernat, T.; Botargues, T.; Cabeza, L.F. Comparative Analysis of Energy Demand and CO2 Emissions on Different Typologies of Residential Buildings in Europe. *Energies* **2019**, *12*, 2436.
18. Ciancio, V.; Salata, F.; Falasca, S.; Curci, G.; Golasi, I.; de Wilde, P. Energy demands of buildings in the framework of climate change: An investigation across Europe.*Sustain. Cities Soc.* **2020**, *60*, 102213.
19. Ciardiello, A.; Rosso, F.; Dell'Olmo, J.; Ciancio, V.; Ferrero, M.; Salata, F. Multi-objective approach to the optimization of shape and envelope in building energy design. *Appl. Energy* **2020**, *280*, 115984.
20. Kheiri, F. A review on optimization methods applied in energy-efficient building geometry and envelope design. *Renew. Sustain. Energy Rev*. **2018**, *92*, 897–920, https://doi.org/10.1016/j.rser.2018.04.080.
21. Yoonseok Shin, Hunhee Cho, Kyung-In Kang. Simulation model incorporating genetic algorithms for optimal temporary hoist planning in high-rise building construction. Automation in Construction, **2011**, *20*, 550–558.
22. Holland, J.H. *Adaptation in Natural and Artificial Systems: An Introductory Analysis with Applications to Biology, Control, and Artificial Intelligence*; MIT Press: Cambridge, MA, USA, 1992.
23. EPBD: Directive 2010/31/EU of the European Parliament and of the Council of 19 May 2010 on the Energy Performance of Buildings (Recast)[EB/OL]. Available online: http: //ec.europa.eu/energy/efficiency/buildings/buildings_en.htm (accessed on 18 June 2010).
24. Ferrara, M.; Fabrizio, E.; Virgone, J.; Filippi, M. A simulation-based optimization method for cost-optimal analysis of nearly Zero Energy Buildings. *Energy Build.* **2014**, *84*, 442–457.
25. Thalfeldt, M.; Pikas, E.; Kurnitski, J.; Voll, H. Facade design principles for nearly zero energy buildings in a cold climate. *Energy Build*. **2013**, *67*, 309–321.
26. Chantrelle, F.P.; Lahmidi, H.; Keilholz, W.; El Mankibi, M.; Michel, P. Development of a multicriteria tool for optimizing the renovation of buildings. *Appl. Energy* **2011**, *88*, 1386–1394.
27. Karaguzel, O.T.; Zhang, R.; Lam, K.P. Coupling of whole-building energy simulation and multi-dimensional numerical optimization for minimizing the life cycle costs of office buildings. *Build. Simul.* **2014**, *7*, 111–121.

28. Prada, A.; Pernigotto, G.; Cappelletti, F.; Gasparella, A.; Jan, L.M. HENSEN. Robustness of multi-objective optimization of building refurbishment to suboptimal weather data. In Proceedings of the International High Performance Building Conference, Purdue, IN, USA, 14–17 July 2014.
29. Pernigotto, G.; Prada, A.; Cappelletti, F.; Gasparella, A. Impact of Reference Years on the Outcome of Multi-Objective Optimization for Building Energy Refurbishment. *Energies* **2017**, *10*, 1925.
30. Ascione, F.; Bianco, N.; De Stasio, C.; Mauro, G.M.; Vanoli, G.P. Multi-stage and multi-objective optimization for energy retrofitting a developed hospital reference building: A new approach to assess cost-optimality. *Appl. Energy* **2016**, *174*, 37–68.
31. Asl, M.R.; Zarrinmehr, S.; Bergin, M.; Yan, W. BPOpt: A framework for BIM-based performance optimization. *Energy Build.* **2015**, *108*, 401–412.
32. Echenagucia, T.M.; Capozzoli, A.; Cascone, Y.; Sassone, M. The early design stage of a building envelope: Multi-objective search through heating, cooling and lighting energy performance analysis. *Appl. Energy* **2015**, *154*, 577–591.
33. Bre, F.; Silva, A.S.; Ghisi, E.; Fachinotti, V. Residential Building Design Optimisation Using Sensitivity Analysis and Genetic Algorithm. *Energy Build.* **2016**, *133*, 853–866.
34. Toutou, A. A Parametric Approach for Achieving Optimum Residential Building Performance in Hot Arid Zone. Master's Thesis, Alexandria University, Alexandria, Egypt, 2018.
35. Gagnon, R.; Gosselin, L.; Decker, S.A. Performance of a sequential versus holistic building design approach using multi-objective optimization. *J. Build. Eng.* **2019**, *26*, 100883.
36. Li, Y.; Bonyadi, N.; Papakyriakou, A.; Lee, B. A hierarchical decomposition approach for multi-level building design optimization. *J. Build. Eng.* **2021**, *44*, 103272.
37. Zhang, T.; Wang, D.; Liu, H.; Liu, Y.; Wu, H. Numerical investigation on building envelope optimization for low-energy buildings in low latitudes of China. *Build. Simul.* **2020**, *13*, 257–269. https://doi.org/10.1007/s12273-019-0577-6.
38. Li, Z.; Tian, M.; Zhao, Y.; Zhang, Z.; Ying, Y. Development of an Integrated Performance Design Platform for Residential Buildings Based on Climate Adaptability. *Energies* **2021**, *14*, 8223. https://doi.org/10.3390/en14248223.
39. Xu, Y.; Zhang, G.; Yan, C.; Wang, G.; Jiang, Y.; Zhao, K. A two-stage multi-objective optimization method for envelope and energy generation systems of primary and secondary school teaching buildings in China. *Build. Environ.* **2021**, *204*, 108142.
40. Diamond, R.C.; Ye, Q.; Feng, W.; Yan, T.; Mao, H.; Li, Y.; Guo, Y.; Wang, J. Sustainable Building in China—A Green Leap Forward? *Buildings* **2013**, *3*, 639–6582.
41. Lush, D.; Butcher, K.; Appleby, P. *Environmental Design: CIBSE Guide A*; The Chartered Institution of Building Services Engineers: London, UK, 2006.
42. Ramallo-González, A.P. Modelling, Simulation and Optimisation Methods for Low-Energy Buildings. Ph.D. Thesis, University of Exeter, Stocker, UK, 2013.
43. Shi, L.; Zhang, Y.; Wang, Z.; Cheng, X.; Yan, H. Luminance parameter thresholds for user visual comfort under daylight conditions from subjective responses and physiological measurements in a gymnasium. *Build. Environ.* **2021**, *205*, 108187.
44. *ASHRAE Handbook Fundamentals*; American Society of Heating, Refrigerating and Air-Conditioning Engineers: Atlanta, GA, USA, 2009.
45. Pedersen, C.O.; Fisher, D.E.; Liesen, R.J. Development of a heat balance procedure for calculating cooling loads. *ASHRAE Trans.* **1997**, *103*, 459–468.
46. Walton, G.N. *Thermal Analysis Research Program Reference Manual*; National Bureau of Standards: Gaithersburg, MD, USA, 1983.
47. Balali, A.; Valipour, A. Prioritization of passive measures for energy optimization designing of sustainable hospitals and health centres. *J. Build. Eng.* **2020**, *35*, 101992.
48. Nabil, A.; Mardaljevic, J. Useful daylight illuminances: A replacement for daylight factors. *Energy Build.* **2006**, *38*, 905–913.
49. Wang, Y.; Li, C.; Jin, X.; Xiang, Y.; Li, X. Multi-objective optimization of rolling schedule for tandem cold strip rolling based on NSGA-II. *J. Manuf. Process.* **2020**, *60*, 257–267.
50. Gan, Y.; Yang, M.; Sun, F.; Yang, L. A quantitative model and solution of reaction heat for microfluidic chips based on Kriging and NSGA-II. *Thermochim. Acta.* **2020**, *694*, 178803.
51. Liu, D.; Huang, Q.; Yang, Y.; Liu, D.; Wei, X. Bi-objective algorithm based on NSGA-II framework to optimize reservoirs operation. *J. Hydrol.* **2020**, *585*, 124830.
52. Delgarm, N.; Sajadi, B.; Delgarm, S.; Kowsary, F. A novel approach for the simulation-based optimization of the buildings energy consumption using NSGA-II: Case study in Iran. *Energy Build.* **2016**, *127*, 552–560.
53. Zhou, Y.; Cao, S.; Kosonen, R.; Hamdy, M. Multi-objective optimisation of an interactive buildings-vehicles energy sharing network with high energy flexibility using the Pareto archive NSGA-II algorithm. *Energy Convers. Manag.* **2020**, *218*, 113017.
54. Yusoff, Y.; Ngadiman, M.S.; Zain, A.M. Overview of NSGA-II for Optimizing Machining Process Parameters. *Procedia Eng.* **2011**, *15*, 3978–3983.
55. Roman, N.D.; Bre, F.; Fachinotti, V.D.; Lamberts, R. Application and characterization of metamodels based on artificial neural networks for building performance simulation: A systematic review. *Energy Build.* **2020**, *217*, 109972.
56. Buratti, C.; Orestano, F.C.; Palladino, D. Comparison of the Energy Performance of Existing Buildings by Means of Dynamic Simulations and Artificial Neural Networks. *Energy Procedia* **2016**, *101*, 176–183.
57. Magnier, L.; Haghighat, F. Multiobjective optimization of building design using TRNSYS simulations, genetic algorithm, and Artificial Neural Network. *Build. Environ.* **2010**, *45*, 739–746.

58. Neto, A.H.; Fiorelli, F.A.S. Comparison between detailed model simulation and artificial neural network for forecasting building energy consumption. *Energy Build.* **2008**, *40*, 2169–2176.
59. Mukhamet, T.; Kobeyev, S.; Nadeem, A.; Memon, S.A. Ranking PCMs for building façade applications using multi-criteria decision-making tools combined with energy simulation. *Energy* **2021**, *215 Pt B*, 119102.